WORKING paper

BANQUE DE FRANCE
EUROSYSTÈME

The Shadow Rate Model: Let's Make it Real!

Adam Golinski[1], Sophie Guilloux-Nefussi[2] and Jean-Paul Renne[3]

October 2025, WP #1014

ABSTRACT

This paper expands upon conventional shadow rate models, which typically concentrate on the term structure of nominal yields, by integrating real interest rates. Close to zero-lower bound periods, real rates inherit part of the non-linearity stemming from the constraints that apply to nominal rates. We introduce a specific macro-finance adaptation of our real/nominal shadow rate model and apply it to U.S. data spanning the last five decades. We exploit the model to calculate real and nominal term premiums and to examine how the dynamic responses of real and nominal rates to economic shocks are constrained during zero-lower bound periods.

Keywords: Shadow Rate, Real and Nominal Risk Premiums, Yield Curve.

JEL classification: E31, E43, E52, E58, G12

[1] Banque de France and University of York, adam.golinski@banque-france.fr.
[2] Banque de France, sophie.guilloux-nefussi@banque-france.fr.
[3] University of Lausanne, Faculty of Business and Economics (HEC Lausanne), jean-paul.renne@unil.ch.
We are grateful to Christoph Grosse Steffen, Demetris Koursaros (discussant), Jean-Stéphane Mésonnier, Dora Xia (discussant) for useful comments and discussions. We also thank participants at the Banque de France seminar series, the 2025 annual conference of the Society for Financial Econometrics, the 2025 Financial Management and Accounting Research meeting, the annual conference of the International Association for Applied Econometrics (2025), the 2025 RCEA International Conference in Economics, Econometrics, and Finance.

NON-TECHNICAL SUMMARY

Since the late 2000s, after many central banks hit the lower bound on policy rates in the wake of the Global Financial Crisis, shadow-rate models of the yield curve—building on the original idea of Black (1995)—have gained prominence. These models address situations where policy rates cannot fall further, even though economic forces would push them lower. Although recent inflation has led to higher rates, the risk of returning to very low yields remains, especially given the long-term decline in the natural rate of interest driven by slower productivity growth, demographic changes, and rising inequality. This makes it essential to use yield curve models that account for lower-bound constraints.

This paper extends the traditional shadow-rate framework, which typically focuses only on nominal yields, by incorporating real (inflation-adjusted) interest rates. Real rates are central to household and corporate decisions about saving, borrowing, and investment, and they play a key role in asset valuation. Modeling nominal and real yields jointly also makes it possible to study the dynamics of inflation compensation (the difference between the two), which reflects investors' expectations of future inflation. We propose approximation techniques to price inflation-linked securities alongside nominal ones within a unified shadow-rate model.

We apply this framework to U.S. data spanning the past fifty years, allowing us to examine how nominal and real term premiums evolve and how the dynamics of yields change when monetary policy is constrained by the zero lower bound (ZLB). A central insight is that the probability of being stuck at the ZLB is highly sensitive to the level of the equilibrium nominal short-term interest rate. When this equilibrium rate is relatively high—for example, 4 percent—the chance of hitting the lower bound is modest (around 5 percent). But when it falls to 2.5 percent, the probability roughly doubles to 10 percent (see the figure below). This finding underscores how a low natural rate environment amplifies the risk of ZLB episodes.

Figure 1. Conditional probabilities of being in the lower-bound regime

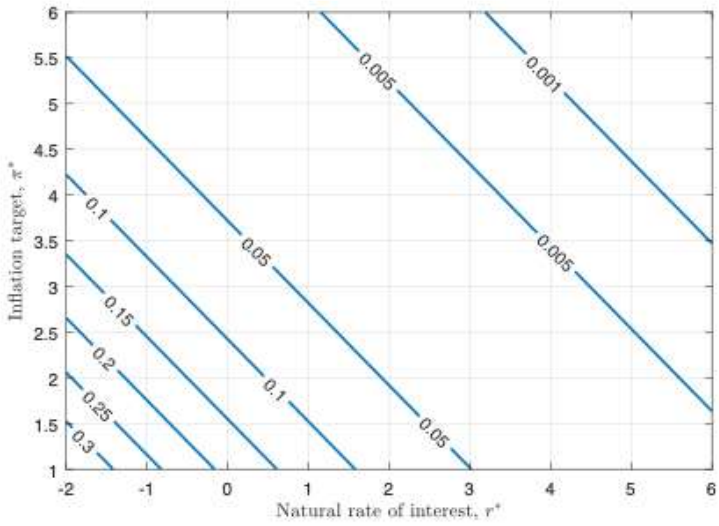

Note: This figure illustrates the influence of the natural rate of interest (r^*) and of the inflation target (π^*) on the frequency of lower-bound regimes. Specifically, the blue curves show combinations of r^* and π^* that yield a given conditional probability (labeled on each curve) of being in the lower-bound regime.

Overall, the paper demonstrates that extending shadow-rate models to include both nominal and real yields provides a richer understanding of bond market dynamics under policy constraints. It highlights how secular trends in the natural rate of interest make economies more exposed to the lower bound, and why tools that account for these risks are essential for policymakers and market participants alike.

Le modèle « shadow rate » :

Rendons le réel !

RÉSUMÉ

Cet article élargit le cadre des modèles de taux d'intérêt implicite (dit « shadow rate ») conventionnels, qui se concentrent généralement sur la structure par terme des rendements nominaux, en y intégrant les taux d'intérêt réels. Lorsque les taux nominaux sont à proximité de leur borne inférieure (zéro), les taux réels héritent d'une partie de la non-linéarité découlant des contraintes qui s'appliquent aux taux nominaux. Nous estimons une version macro-financière de notre modèle de shadow rate nominal/réel sur des données américaines couvrant les cinq dernières décennies. Nous exploitons ce modèle pour calculer les primes de terme réelles et nominales et pour analyser la manière dont les réactions dynamiques des taux réels et nominaux aux chocs économiques sont affectées lors des périodes de plancher zéro.

Mots-clés : modèle « shadow rate », primes de risque nominale et réelle, courbe de taux d'intérêt.

---

1. Introduction

Since the late 2000s, after many central banks hit the lower bound on policy rates in the wake of the Global Financial Crisis, shadow-rate models of the yield curve—building on the original idea of Black (1995)—have gained considerable prominence. Although recent inflationary pressures have compelled central banks to gradually raise interest rates, the potential for returning to extremely low yields in the future remains a plausible scenario, especially in a context of declining natural rate of interest.[1] As a result, it is important to have term structure models that adequately accommodate and address the constraints posed by their lower bounds.

This paper extends traditional shadow-rate models, which typically focus solely on nominal yields, by incorporating real interest rates. Real interest rates, representing the inflation-adjusted cost of borrowing or lending, are crucial for economic decisions and asset valuations. The joint modeling of nominal and real yield curves allows, in particular, for an investigation into the dynamics of the break-even inflation rate (or inflation compensation), defined as the difference between the two curves.

Any model of the term structure of nominal yields that features a nominal stochastic discount factor and inflation—including the shadow rate models of Wu and Xia (2016) or Wu and Zhang (2019)—also imply the term structure of real rates (see, e.g., Gürkaynak and Wright, 2012). The latter are, however, not considered in the context of shadow rate models because the computation of real rates then involves conditional expectations that are more general than the ones needed to price nominal yields. Approximations to this type of conditional expectations have been recently proposed in the credit-risk context by Pallara and Renne (2024) and Renne and Pallara (2023), who extend the formulas originally proposed by Wu and Xia (2016). In the present paper, we show how to adapt these approximations to price inflation-linked bonds and thus to derive real yield curves.

We propose an application that exploits these formulae to build a macro-finance model that captures the joint dynamics of macroeconomic variables, real and nominal yields. We

[1] Over the past decade, economists and policymakers have increasingly recognized a significant decline in the average natural rate of interest. This decline is attributed to factors such as lower productivity growth, demographic shifts, increased inequality, and heightened uncertainty, indicating that the downward trend in the natural rate of interest is likely to persist(see, e.g., Rachel and Summers, 2019; Bielecki et al., 2023).

bring this model to U.S. data covering the last fifty years. The model is exploited to compute real and nominal term premiums, and to analyse how the dynamic reactions of real and nominal rates to economic shocks are constrained during zero-lower bound (ZLB) periods. The model incorporates the natural interest rate (r_t^*) and inflation target rate (π_t^*), enabling analysis of how changes in the equilibrium nominal short-term interest rate ($i_t^* = r_t^* + \pi_t^*$) affect yield dynamics and frequency of ZLB events. Our findings show a significant increase in the probability of a ZLB regime as the equilibrium nominal rate falls; for example, the ZLB probability increases from 5% at $i_t^* = 4\%$ to 10% at $i_t^* = 2.5\%$.

The present article relates to the literature that develops and investigates ZLB-consistent models. Four main approaches stand out: (i) quadratic term structure models, or QTSM (QTSM hereinafter, e.g, Ahn et al., 2002; Andreasen and Meldrum, 2019; Leippold and Wu, 2002), (ii) models based on square-root processes (or CIR processes, e.g., Cox et al., 1985; Pearson and Sun, 1994; Dai and Singleton, 2000), (iii) models based on auto-regressive gamma processes (ARG processes, e.g., Gouriéroux and Jasiak, 2006; Dai et al., 2010; Monfort et al., 2017; Roussellet, 2023), and (iv) shadow-rate models. The first three types provide closed-form bond pricing formulas and positive heteroskedastic yields. Nevertheless, explicitly incorporating macroeconomic variables into these models is challenging as strong constraints apply to the factors' dynamics for nominal rates to remain non-negative. For instance, in the context of QTSM, the short-term nominal rate (i_t) is a quadratic function of $\mathbf{x}_t$, that follows a Gaussian vector autoregressive model (VAR). Assume inflation (π_t) is one of $\mathbf{x}_t$'s components and consider a value of $\mathbf{x}_t$ that is such that i_t is at the lower bound, i.e., $i = 0$. Everything else equal, i_t is a quadratic function of π_t around that point. As a result, for very low values of i_t, both a unit increase or a unit decrease in π_t, everything else equal, have approximately the same *positive* impact on i_t in a QTSM model. With regard to CIR or ARG processes, limitations arise from the fact that in these models factors are all non-negative and positively correlated with each other. While these constraints are not necessarily a problem if the factors are la-

tent, they become very strong and limiting if some of the factors are explicitly recognized as macroeconomic factors—typically inflation.[2,3]

The shadow-rate model has been adopted by numerous studies (e.g., Ichiue and Ueno, 2007, 2013; Kim and Singleton, 2012; Krippner, 2013; Priebsch, 2013; Kim and Priebsch, 2013; Lemke and Vladu, 2017; Bauer and Rudebusch, 2016; Christensen and Rudebusch, 2015, 2016; Wu and Xia, 2016, 2020; Goliński and Spencer, 2024).[4] In this framework, the short-term interest rate is defined as the maximum of zero and of the so-called shadow rate. ZLB periods occur when the shadow rate turns negative. The model can generate prolonged periods of ZLB, contrary to quadratic and square-root approaches, that treat the lower bound as a reflecting barrier. While this feature is also achieved by the auto-regressive gamma zero process introduced by Monfort et al. (2017), a key advantage of the shadow-rate model—over all other lower-bound-consistent models—is its flexibility regarding the correlation structure of the pricing factors. This makes it particularly well-suited when one wants to combine the dynamics of macro-economic factors with those of interest rates.

To our knowledge, two other papers tackle the pricing of both nominal and inflation-linked bonds in the context of shadow-rate model, namely Imakubo and Nakajima (2015) and Carriero et al. (2018). To obtain tractable pricing formulas, the authors of these two papers proceed by positing both the nominal and the real stochastic discount factors, using standard specifications for each of them. Since the ratio of the two SDFs is the gross growth rate of the price index, doing so fully constrain the inflation dynamics, that then turn out to be highly nonlinear in the pricing factors. This complicates the use of inflation and of inflation forecasts when it comes to estimating these models—inflation is absent from the empirical analyses of

[2] Roussellet (2023) proposes a model that combines components of the ARG and QTSM frameworks that kills the necessity to have positively correlated factors. The specifications however also imply constraints on the relationships between nominal rates and macroeconomic factor. In particular, this framework also faces the type of limitation mentioned above for the QTSM: periods of low i_t correspond to periods where a quadratic function of the factors $\mathbf{x}_t$ is close to its minimum (zero), which implies that, everything else equal, the derivative of i_t to π_t—or any other variable—is then zero.

[3] CIR and standard ARG models treat the ZLB as a reflecting barrier and, in these frameworks, the probability of having an unchanged short-term rate for two subsequent periods is zero. Monfort et al. (2017) extend the standard ARG models to allow factors for stay at zero for stochastic periods of time. In this framework, however, the factors are all non-negative and positively correlated with each other.

[4] When contrasting shadow-rate arbitrage-free Nelson-Siegel (AFNS) models with their standard Gaussian counterparts using Japanese term structure data, Christensen and Rudebusch (2015) observe that shadow-rate models offer better in-sample fits and can capture yield dynamics at the Zero Lower Bound (ZLB). Similar evidence was found for U.S. yield data by Christensen and Rudebusch (2016).

Imakubo and Nakajima (2015) and Carriero et al. (2018)—which limits the possibilities of model validation and prevents from using inflation surveys at the estimation stage.[5]

Through our application, our study relates to the literature on the interactions between the yield curve and macroeconomy. Seminal contribution in this respect include Ang and Piazzesi (2003), Dewachter and Lyrio (2006), Hördahl et al. (2006), Diebold et al. (2006), Rudebusch and Wu (2008), and Joslin et al. (2014). A strand of this literature focuses on the joint modeling of nominal and real yield curves (Campbell and Viceira, 2001; Evans, 2003; Ang et al., 2008; Christensen et al., 2010; Chernov and Mueller, 2012; Hördahl and Tristani, 2012; Breach et al., 2020; Bletzinger et al., 2025). These papers are however not consistent with the existence of a lower bound for nominal interest rates.

Our paper also touches upon the literature on the probability of reaching the zero lower bound (ZLB) and its relation to equilibrium interest rates. Chung et al. (2012) find that pre-Great Recession research underestimated the probability of reaching the ZLB because it failed to account for parameter and latent variable uncertainty in the model. Sims and Wu (2020) examine the increasing likelihood of the ZLB recurring, given the secular decline in the natural interest rate. Bianchi et al. (2021) demonstrate how deflationary bias emerges when the probability of reaching the ZLB is non-zero. Fernández-Villaverde et al. (2023) find that the probability of reaching the ZLB increases when the inflation target is low and wealth inequality is high. They find that lowering the inflation target make ZLB events more likely.

The remainder of the paper is structured as follows. Section 2 discusses the challenges associated with pricing inflation-linked bonds in the context of shadow-rate models, along with the introduction of approximate pricing formulas. Section 3 introduces a specific version of a real/nominal shadow-rate model and estimates it using U.S. data. Section 5 concludes. The Appendix contains technical results. Proofs are gathered in the Online Appendix.

2. The general nominal-real shadow rate model

This section present the specification of our nominal-real shadow rate model. The ingredients are the following: the link between the short-term nominal rate i_t and the shadow rate s_t (eq. 1), the link between the shadow rate and the state vector $\mathbf{x}_t$ (eq. 2), the dynamics of $\mathbf{x}_t$

[5]The importance of using inflation surveys when estimating the joint dynamics of real and nominal term premiums is illustrated, e.g., by Chernov and Mueller (2012) and Breach et al. (2020).

(eq. 3), the specification of the stochastic discount factor (eqs. 4 and 5), and the link between inflation and the state vector (eq. 10). While we consider standard specifications for each of these ingredients, we highlight that they jointly imply that the prices of inflation-linked bond take the form of conditional expectations that are more general than those associated with nominal bonds, which has not been discussed and solved earlier in the literature. Let us be more specific.

The short-term nominal risk-free rate is given by:[6]

$$i_t = \max(\underline{i}, s_t), \tag{1}$$

where $\underline{i}$ is the effective lower bound and s_t is the shadow rate affine in the state vector $\mathbf{x}_t$:

$$s_t = \delta_0 + \boldsymbol{\delta}_1' \mathbf{x}_t. \tag{2}$$

The state vector follows a Gaussian VAR:

$$\mathbf{x}_t = \boldsymbol{\mu} + \boldsymbol{\Phi}\mathbf{x}_{t-1} + \boldsymbol{\Sigma}\boldsymbol{\varepsilon}_t, \quad \boldsymbol{\varepsilon}_t \sim \ i.i.d. \mathcal{N}(\mathbf{0}, \boldsymbol{I}), \tag{3}$$

where $\mathbf{0}$ denotes a vector of zeros and $\boldsymbol{I}$ is a conformable identity matrix.

The nominal stochastic discount factor (SDF) is given by:

$$\mathcal{M}_{t,t+1} = \exp\left(-i_t + \boldsymbol{\lambda}_t' \boldsymbol{\varepsilon}_{t+1} - \frac{1}{2}\boldsymbol{\lambda}_t'\boldsymbol{\lambda}_t\right), \tag{4}$$

where the vector of prices of risk, $\boldsymbol{\lambda}_t$, is affine in $\mathbf{x}_t$:

$$\boldsymbol{\lambda}_t = \boldsymbol{\lambda}_0 + \boldsymbol{\Lambda}_1' \mathbf{x}_t. \tag{5}$$

Under eqs. (3) to (5), it is well-known that the risk-neutral dynamics of $\mathbf{x}_t$ are given by (e.g., Ang and Piazzesi, 2003):

$$\mathbf{x}_t = \boldsymbol{\mu}^{\mathbb{Q}} + \boldsymbol{\Phi}^{\mathbb{Q}}\mathbf{x}_{t-1} + \boldsymbol{\Sigma}\boldsymbol{\varepsilon}_{t+1}^{\mathbb{Q}}, \quad \boldsymbol{\varepsilon}_{t+1}^{\mathbb{Q}} \sim \mathcal{N}^{\mathbb{Q}}(\mathbf{0}, \boldsymbol{I}), \tag{6}$$

[6]While the effective lower bound $\underline{i}$ is generally considered to be zero in the US, the European Central Bank (ECB) has ventured into negative territory with its deposit facility rate, effectively pulling short-term interest rates into negative territory as well. This implies that $\underline{i}$ has at times been negative in the Euro Area. The ECB deposit facility rate reached a low of -0.5% in September 2019 and remained there for several years. Wu and Xia (2020) introduce a model incorporating an ELB that is stochastic, and recognized as such by market participants. The model is estimated on eurozone data, and their results suggest that the ELB process explains a modest share of the observed term premium (see their Figure 10).

with

$$\boldsymbol{\mu}^{\mathbb{Q}} = \boldsymbol{\mu} + \boldsymbol{\Sigma}\boldsymbol{\lambda}_0, \quad \boldsymbol{\Phi}^{\mathbb{Q}} = \boldsymbol{\Phi} + \boldsymbol{\Sigma}\boldsymbol{\Lambda}_1'. \tag{7}$$

Further, the prices of nominal bonds are given by:

$$\begin{aligned} B_{t,h} &= \mathbb{E}_t^{\mathbb{Q}}\left[\exp(-i_t - \cdots - i_{t+h-1})\right] \\ &= \mathbb{E}_t^{\mathbb{Q}}\left[\exp(-\max(\underline{i}, s_t) - \cdots - \max(\underline{i}, s_{t+h-1}))\right]. \end{aligned} \tag{8}$$

Because the short-term nominal rate i_t is not affine in $\mathbf{x}_t$, the standard machinery of affine term structure model cannot be used to compute the previous conditional expectations. Several approaches have then been proposed to approximate for the latter conditional expectation (e.g., Krippner, 2012; Priebsch, 2013; Wu and Xia, 2016). The present study utilizes the approach developed by Wu and Xia (2016), but extends it to accommodate the pricing of inflation-linked bonds, which requires a different form of conditional expectation than that used for nominal bonds in eq. (8), as demonstrated in what follows.

To price real (or inflation-linked bonds), we need to consider the real SDF. The latter relates to the nominal SDF through:[7]

$$\mathcal{M}^r_{t,t+1} = \mathcal{M}_{t,t+1} \exp(\pi_{t+1}), \tag{9}$$

where π_t is the continuously-compounded inflation rate between dates $t-1$ and t. It is usual to consider an inflation rate that is affine in the state vector $\mathbf{x}_t$:

$$\pi_t = \gamma_0 + \boldsymbol{\gamma}_1' \mathbf{x}_t. \tag{10}$$

Eq. (9) shows that the nominal SDF, the real SDF, and the dynamics of inflation cannot be chosen independently. In the present case, the real SDF is determined once (i) the nominal SDF is as in eq. (4) and (ii) inflation is as in eq. (10).

[7] Indeed, consider an asset whose real payoff on date $t+1$ is p_{t+1}. Its nominal payoff will then be $p_{t+1}\exp(\pi_{t+1})$ on date $t+1$. That implies that its date-t price has to be $\mathbb{E}_t[\mathcal{M}_{t,t+1}\exp(\pi_{t+1})p_{t+1}]$ and, in turn, that the real SDF is $\mathcal{M}_{t,t+1}\exp(\pi_{t+1})$. See also Campbell et al. (1997), Chapter 11.

According to eq. (9), the prices of real, or inflation-linked, bonds are given by:[8]

$$\begin{aligned} B^r_{t,h} &= \mathbb{E}^{\mathbb{Q}}_t \left[\exp(-i_t - \cdots - i_{t+h-1} + \pi_{t+1} + \ldots \pi_{t+h})\right] \\ &= \mathbb{E}^{\mathbb{Q}}_t \left[\exp(-\max(\underline{i}, s_t) - \cdots - \max(\underline{i}, s_{t+h-1}) + \pi_{t+1} + \ldots \pi_{t+h})\right]. \end{aligned} \tag{11}$$

This conditional expectation is not of the standard (shadow-rate) type, since its combines, in the exponential, terms of the form $\max(\underline{i}, \delta_0 + \delta_1' \mathbf{x}_{t+k})$ and others that are simply affine in $\mathbf{x}_t$, namely $\gamma_0 + \gamma_1' \mathbf{x}_{t+k}$. The standard formula provided by Priebsch (2013) and Wu and Xia (2016) do not allow to compute these conditional expectations. (They accommodate only terms involving the max operator, not max/affine combinations.) An approximation formula that extends that of Wu and Xia (2016) is, however, proposed by Pallara and Renne (2024) and Renne and Pallara (2023) in the context of credit-risk modelling; this approximation formula is presented in Lemma 1 (see Appendix A). This formula allows to approximate the conditional expectations appearing in eq. (11) with the closed-form expression:[9]

$$B^r_{t,h} \approx \exp(-F_{0,1,t} - F_{1,2,t} - \cdots - F_{h-1,h,t}),$$

[8] Inflation-linked bonds typically include a deflation option: while the principal is indexed to the price index, in the event of deflation (a decrease in the price index) between issuance and maturity, investors are guaranteed to receive at least the original par value at maturity. This offers protection against deflation, ensuring that the principal is not lost even if prices fall (e.g., Grishchenko et al., 2016). Such an embedded option is not considered in equation (11). As demonstrated by Christensen et al. (2016), the value of this deflation option is generally low and thus has a negligible impact on bond prices, particularly for older bonds that have accumulated positive inflation since issuance and for which the option is effectively out-of-the-money. However, the effect is less negligible for "young" bonds during periods of high deflation risk, such as the Great Financial Crisis. To account for this, along with other potential crisis effects, we increase the measurement errors on real yields during the GFC and COVID-19 crisis periods (see Section 4.2).

[9] As mentioned in the introduction, two papers (Imakubo and Nakajima, 2015, and Carriero et al., 2018) circumvent this computational issue by positing that the real SDF is of the form: $\mathcal{M}^r_{t,t+1} = \exp\left(-r_t + \lambda^{r\prime}_t \varepsilon_{t+1} - \lambda^{r\prime}_t \lambda^r_t/2\right)$. In that case, they obtain that the prices of real bonds are exponential affine in $\mathbf{x}_t$, using the standard GTSM formulas. However, since their nominal SDF is given in eq. (4), they have no choice in the inflation process, which, given eqs. (4) and (9), and the previous expression for the real SDF, is (implicitly) equal to:

$$\pi_{t+1} = \log(\mathcal{M}^r_{t,t+1}/\mathcal{M}_{t,t+1}) = i_t - \lambda_t{}'\varepsilon_{t+1} + \frac{1}{2}\lambda_t{}'\lambda_t - r_t + \lambda^{r\prime}_t \varepsilon_{t+1} - \frac{1}{2}\lambda^{r\prime}_t \lambda^r_t.$$

Inflation is then non-linear in $\mathbf{x}_t$, notably because it involves the max operator through i_t. It also comprises quadratic terms in $\mathbf{x}_t$ (through $\lambda_t{}'\lambda_t$ and $\lambda^{r\prime}_t \lambda^r_t$).

with

$$F_{n-1,n,t} = \underbrace{\underline{i} + \sigma_n g\left(\frac{a_n + \mathbf{b}_n' \mathbf{x}_t - \underline{i}}{\sigma_n}\right)}_{\text{nominal forward rate}} - \underbrace{(\dot{c}_n + \mathbf{c}_n' \mathbf{x}_t)}_{\text{inflation discount}} + \underbrace{\Phi^{\mathcal{N}}\left(\frac{\bar{a}_n + \mathbf{b}_n' \mathbf{x}_t - \underline{i}}{\sigma_n}\right) \mathbf{b}' \mathbf{\Phi}_n \mathbf{\Sigma}\mathbf{\Sigma}' \mathbf{\Phi}_n' \mathbf{c}_n}_{\text{interest rate - inflation interaction}}, \tag{12}$$

where σ_n, a_n, $\bar{a}_n$, $\mathbf{b}_n$, $\dot{c}_n$, $\mathbf{c}_n$, and $\mathbf{\Phi}_n$, are obtained by using simple recursive formulas (see Appendix A), and where $g(x) = x\Phi^{\mathcal{N}}(x) + \phi^{\mathcal{N}}(x)$, where $\Phi^{\mathcal{N}}$ and $\phi^{\mathcal{N}}$ are the c.d.f. and p.d.f. of a standard normal variable, respectively.

The nominal forward rate—the first component in eq. (12)—is the same as in the shadow rate model of Wu and Xia (2016). The inflation discount term in eq. (12) represents expected inflation along with convexity adjustments. The final term accounts for convexity adjustments related to the interplay between future interest rates and inflation.

3. A macro-finance framework

While eq. (3) that determines the law of motion of the state vector $\mathbf{x}_t$ is general, this section proposes a more specific dynamics for $\mathbf{x}_t$ in the present section. At the core of the model are three standard macroeconomic equations: the Phillips curve connects inflation to the output gap; the Investment-Savings (IS) curve depicts the relationships between short-term real rates and the output gap; the Taylor rule dictates the central bank's response function.

3.1. Macro dynamics

We assume that log GDP (y_t) is made of two components, namely the potential GDP (y_t^*) and the output gap (z_t). Denoting the log growth rate of potential GDP by g_t (i.e, $g_t = \Delta y_t^*$), we obtain the following expression for the log GDP growth rate:

$$\Delta y_t = g_t + z_t - z_{t-1}. \tag{13}$$

Following Wu and Zhang (2019), we assume that the short-term shadow rate follows a generalized Taylor rule (see, e.g., Orphanides, 2007):

$$s_t = (1 - \rho_i) s_{t-1} + \rho_i [r_t^* + \pi_t^* + \alpha_\pi (\pi_t - \pi_t^*) + \alpha_z z_t] + \sigma_i \varepsilon_{i,t}, \tag{14}$$

with $\varepsilon_{i,t} \sim \ i.i.d. \mathcal{N}(0,1)$, and where $\bar{\pi}_t$, π_t^* and r_t^* are, respectively, the persistent component of inflation (excluding volatile shocks), the inflation target, and the natural rate of interest. Wu and Zhang (2019) show that using the shadow rate instead of the effective short-term rate in the context of small-scale macroeconomic models constitutes a tractable way to capture the effects of non-conventional monetary policy that are implemented during ZLB spells. To this end, Wu and Zhang (2019) propose to combine the previous Taylor rule with an IS curve featuring the shadow rate, whose objective is to summarize the effect of unconventional monetary policy on the economy. Specifically, our IS curve reads:

$$z_t = \rho_z z_{t-1} - \alpha(s_{t-1} - \mathbb{E}(\pi_t|\mathcal{I}_{t-1}) - r_{t-1}^*) + \sigma_z \varepsilon_{z,t}, \tag{15}$$

where $\varepsilon_{z,t} \sim \ i.i.d. \mathcal{N}(0,1)$.

As in Laubach and Williams (2003) and Holston et al. (2017), we tie the natural rate of interest to the potential growth rate:

$$r_t^* = \theta g_t + \kappa_t, \tag{16}$$

where θ corresponds to the risk aversion parameter and κ_t corresponds to the pure preference for present in the context of a Ramsey rule. The latter component is assumed to be time-varying and follows:

$$\kappa_t = \mu_\kappa + \rho_\kappa \kappa_{t-1} + \sigma_\kappa \varepsilon_{\kappa,t}. \tag{17}$$

The inflation target and potential growth rates follow autoregressive processes:

$$\pi_t^* = (1-\rho^*)\mu^* + \rho^* \pi_{t-1}^* + \sigma^* \varepsilon_t^*, \tag{18}$$

$$g_t = (1-\rho_g)\mu_g + \rho_g g_{t-1} + \sigma_g \varepsilon_{g,t}, \tag{19}$$

with $\varepsilon_t^*, \varepsilon_{g,t} \sim \ i.i.d. \mathcal{N}(0,1)$.

Inflation π_t has two components. The first component, $\bar{\pi}_t$, is a persistent factor, whose dynamics take the form of a Phillips curve, with a long-term value that depends on the inflation target π_t^*. The second component, u_t, is more volatile and captures short-living deviations from the persistent trend; we assume that it follows a moving average process (with a small

order p):

$$\pi_t = \bar{\pi}_t + u_t, \tag{20}$$

$$\bar{\pi}_t = (1-\bar{\rho})\pi_t^* + \bar{\rho}\bar{\pi}_{t-1} + \beta z_{t-1} + \sigma_\pi \varepsilon_{\pi,t}, \tag{21}$$

$$u_t = a_0\varepsilon_{u,t} + a_1\varepsilon_{u,t-1} + \cdots + a_p\varepsilon_{u,t-p}, \tag{22}$$

with $\varepsilon_{\pi,t}, \varepsilon_{u,t} \sim$ *i.i.d.* $\mathcal{N}(0,1)$.

3.2. Prices of risk and stochastic discount factor

We introduce an additional state variable, denoted by w_t, which aims to capture the fluctuations in prices of risk. We adopt the following parsimonious formulation for the vector of prices of risk (eq. 5):

$$\boldsymbol{\lambda}_t = \boldsymbol{\lambda}_0 + \boldsymbol{\lambda}_{1,w} w_t, \tag{23}$$

where $\boldsymbol{\lambda}_0$ and $\boldsymbol{\lambda}_{1,w}$ are vectors of dimensions $n_\varepsilon \times 1$, where n_ε is the dimension of the vector of shocks affecting the economy: $\boldsymbol{\varepsilon}_t = [\varepsilon_{i,t}, \varepsilon_{g,t}, \varepsilon_{z,t}, \varepsilon_t^*, \varepsilon_{\pi,t}, \varepsilon_{u,t}, \varepsilon_{w,t}, \varepsilon_{\kappa,t}]'$. Although w_t is the sole driver of the price of risk, it can be correlated with other variables. Indeed, its dynamics are expressed as follows:

$$w_t = (1-\rho_w)\mu_w + \rho_w w_{t-1} + \sigma_w \varepsilon_{w,t} + \sigma_{w,z}\varepsilon_{z,t} + \sigma_{w,\pi}\varepsilon_{\pi,t} + \sigma_{w,g}\varepsilon_{g,t}, \tag{24}$$

where $\varepsilon_w \sim$ *i.i.d.* $\mathcal{N}(0,1)$. Notice that while the shock $\varepsilon_{w,t}$ is specific to w_t, this variable is also impacted by $\varepsilon_{z,t}$, $\varepsilon_{\pi,t}$, and $\varepsilon_{g,t}$.

4. Empirical implementation

4.1. Data

The model can be cast into a state-space form whose transition equations correspond to the Gaussian VAR followed by the state vector $\mathbf{x}_t$ (i.e., eq 3), and whose measurement equations involve macroeconomic variables, nominal and real yields, as well as survey-based forecasts. Since interest rates are nonlinear functions of $\mathbf{x}_t$, some measurement equations are not affine. Accordingly, we employ the Extended Kalman Filter (EKF) to estimate the model.[10]

[10] Most studies choose the EKF to estimate shadow-rate models. Christensen and Rudebusch (2015) compare the extended Kalman filter with the unscented Kalman filter using Japanese yield data and found minimal differences; they favor the EKF due to its lower computational intensity.

The measurement equations and the data they involve are as follows:

- **Macroeconomic variables (4 variables)**: Inflation (eq. 20) is the monthly log growth rate of the price index (CPIAUCSL series in the FRED database). Real activity (eq. 13) is measured by the monthly GDP growth index constructed by Brave et al. (2019). The output gap (eq. 15) is calculated as the relative deviation between quarterly GDP and an estimate of the potential GDP (series GDPC1 and GDPPOT in FRED). Furthermore, we use the measure of perceived inflation target (PTR) used in the FRB/US model (Brayton et al., 2014) to anchor our π_t^* estimate (eq. 18).[11] The output gap and PTR are available on a quarterly basis; we convert them into monthly time series, filling missing values with the last available observation.

- **Nominal and real yields (11 variables)**: The financial block consists of nominal yields with maturities of 3 months, 1, 2, 3, 5, 7, and 10 years, and of real yields based on TIPS, with maturities of 2, 5, 7, and 10 years. Except for the 3-month nominal yield (series DTB3 in FRED), nominal yields are taken from the updated Gürkaynak et al. (2007) database. Real yields come from the updated Gürkaynak et al. (2010) database. Given the relatively recent introduction of TIPS, we supplement our dataset with backcasted 10-year real rates from Groen and Middeldorp (2013), who estimate these rates by regressing TIPS yields on an extensive array of over 100 macroeconomic and financial variables, employing partial least squares to guide the variable selection process.[12]

- **Survey-based forecasts (6 variables)**: Among the observed variables we also incorporate survey-based forecasts. This approach, popularized by Kim and Wright (2005) and Kim and Orphanides (2012), aims at capturing better the typically high persistence in the estimation of term structure models (e.g., Jardet et al., 2013; Bauer et al., 2012). We consider 1-year-ahead and 10-years-ahead survey-based forecasts of average inflation and the average short-term interest rate. These surveys are taken from the quarterly Survey of Professional Forecasters of the Federal Reserve Bank of Philadelphia.

[11] This variable has been used in various academic research, including Bauer and Rudebusch (2020) and Shapiro and Wilson (2022). It is available at https://www.federalreserve.gov/econres/us-models-package.htm.

[12] The estimates of Groen and Middeldorp (2013) are available here.

To place greater emphasis on the long-run surveys during estimation, and considering their slow-moving nature, we convert them into monthly time series, filling missing values with the last available observation.

4.2. Parameters identification and estimation strategy

We estimate the model by maximizing the likelihood function using the extended Kalman filter. Macroeconomic variables, bond yields, and survey-based forecasts are assumed to be observed with measurement errors. Specifically, the measurement equations of the state-space model take the following form:

$$\begin{bmatrix} Macro_t \\ Yields_t \\ Surveys_t \end{bmatrix} = \begin{bmatrix} \mathbf{a}_M + \mathbf{B}_M \mathbf{x}_t \\ \mathcal{Q}(\mathbf{x}_t) \\ \mathcal{S}(\mathbf{x}_t) \end{bmatrix} + \begin{bmatrix} \boldsymbol{\varepsilon}_{M,t} \\ \boldsymbol{\varepsilon}_{Y,t} \\ \boldsymbol{\varepsilon}_{S,t} \end{bmatrix}, \tag{25}$$

where $\boldsymbol{\varepsilon}_{M,t}$, $\boldsymbol{\varepsilon}_{Y,t}$, and $\boldsymbol{\varepsilon}_{S,t}$ are independent Gaussian measurement errors, and where functions $\mathcal{Q}$ and $\mathcal{S}$ are nonlinear functions of $\mathbf{x}_t$. Although these functions are non-linear, they admit analytic derivatives, which facilitates their use in the EKF (see Appendix A for the bond pricing equations, and III for the forecast equations).

We impose a number of constraints on the parameter space to facilitate the estimation and to achieve a satisfying relative fit of the different variables. These constraints are detailed in Appendix B.

4.3. Estimation results

Table 1 presents the model parameterization. To facilitate interpretation, some parameters have been annualized (when applicable, we show the annualization multiplier). The standard errors, displayed in smaller font, are calculated from the inverse of the (numerical) covariance matrix of parameter estimates based on the gradient of the likelihood function of the estimated parameters, excluding the calibrated parameters and those that converged to the boundaries during estimation.[13]

Figure 1 illustrates the model fit of macroeconomic variables. Additional figures, gathered in Supplement V, show the fit of nominal and real interest rates, and of survey-based

[13]These boundaries, and other parameter constraints, are detailed in Appendix B.

Table 1: **Model parameterization**. To facilitate interpretation, some parameters have been annualized (when applicable, we show the annualization multiplier). The standard errors, displayed in smaller font, are calculated from the inverse of the (numerical) covariance matrix of parameter estimates based on the gradient of the likelihood function. Calibrated parameters and those that converged to the boundaries during estimation have been excluded from the calculation of standard errors. We refer to Appendix B for details regarding constraints imposed on the parameter space.

Parameter	Estimate (S.E.)	Multiplier	Parameter	Estimate (S.E.)	Multiplier
Estimated model parameters:					
ρ_i	0.0105 0.0010	$\times 1$	ρ_g	0.7901 0.1058	$\times 1$
σ_g	0.6088 0.0318	$\times 1200$	α	74.6946 22.1453	$\times 100$
ρ_z	0.9464 0.0223	$\times 1$	σ_z	0.4193 0.0086	$\times 100$
ρ^*	0.9950 0.0000	$\times 1$	σ^*	0.0370 0.0011	$\times 1200$
μ_κ	0.0000 0.0000	$\times 1200$	ρ_κ	0.9950 0.0000	$\times 1$
$\bar{\rho}$	-0.3898 0.3447	$\times 1$	β	0.0939 0.0223	$\times 12$
σ_π	0.0109 0.0301	$\times 1200$	$a_{u,1}$	0.0025 0.0001	$\times 1$
$a_{u,2}$	0.0008 0.0001	$\times 1$	ρ_w	0.9286 0.0231	$\times 1$
$\sigma_{w,g}$	0.0933 0.0255	$\times 1$	$\sigma_{w,z}$	0.0000 0.0977	$\times 1$
$\sigma_{w,\pi}$	0.0033 0.1051	$\times 1$			
Calibrated model parameters:					
α_π	1.5000	$\times 1$	α_z	0.5000	$\times 12$
σ_i	0.4176	$\times 1200$	μ_g	2.6532	$\times 1200$
μ^*	4.0259	$\times 1200$	σ_κ	0.1961	$\times 1200$
θ	1.0000	$\times 1$	$\underline{i}$	0.0000	$\times 1$
μ_w	0.0000	$\times 1200$	σ_w	0.2975	$\times 1$
Measurement errors:					
σ_o	0.5000 0.0000	$\times 100$	σ_n	0.3229 0.0059	$\times 1200$
σ_r	0.2429 0.0167	$\times 1200$	$\sigma_{r,liq}$	0.9419 0.0946	$\times 1200$
σ_s	0.2400 0.0000	$\times 1200$	$\sigma_{ptr} = 5 \times \sigma_s$		
$\sigma_{gdp} = \sigma_o/100$			$\sigma_{inf} = \sigma_o/100$		
$\sigma_y = \sigma_s$			$\sigma_{3tb} = \sigma_s/4$		
Price of risk parameters:					
$\lambda_{0,\varepsilon_i}$	0.0775 0.2319		$\lambda_{w,\varepsilon_i}$	0.1536 0.0958	
$\lambda_{0,\varepsilon_g}$	0.2128 0.1084		$\lambda_{w,\varepsilon_g}$	0.2273 0.8148	
$\lambda_{0,\varepsilon_z}$	-1.0851 3.7203		$\lambda_{w,\varepsilon_z}$	-0.1914 0.9255	
$\lambda_{0,\varepsilon^*}$	0.1924 1.2060		$\lambda_{w,\varepsilon^*}$	0.5179 0.3697	
$\lambda_{0,\varepsilon_\pi}$	2.0448 63.8248		$\lambda_{w,\varepsilon_\pi}$	0.5400 7.5356	

forecasts. These figures overall suggest that the model is flexible enough to capture satisfactorily the dynamics of all considered variables. Table 2 reports annualized root mean-square error (RMSE) for nominal and real yields, and for surveys. The average RMSE for nominal yields amounts to 26 basis points, which is reasonable for a macro-based model that does not include yield factors (such as principal components of yield). The fit of real yields is slightly better in normal (i.e., higher liquidity) times, amounting to 23 basis points on average across maturities, but the fit deteriorates substantially during periods of low liquidity to 77 basis points.[14] The RMSEs for inflation and interest rate surveys are about 28 and 15 basis points, respectively. Again, given that the model does not include any yield-based factors, this fit can be considered relatively good and in line with other studies.

Table 2: **Root mean-square fitting errors**. This table shows root mean-square errors for annualized nominal and real yields, and for surveys. RMSEs are expressed in basis points.

Maturities	3m	1y	2y	3y	5y	7y	10y	Average
Yields:								
Nominal yields	55	33	20	16	13	13	29	26
Real yields - high liq.			39		16	13	23	23
Real yields - low liq.			118		97	87	136	110
Surveys:								
Inflation rate		31					26	28
3m T-bill rate		17					13	15

A byproduct of the estimation is the natural rate of interest (hence NRI), which we plot in Figure 2, together with the estimates from Laubach and Williams (2003) and Holston et al. (2017). While our NRI exhibits broad fluctuations consistent with the estimates in Laubach and Williams and Holston et al., it is more volatile. In particular, it exhibits negative values over a substantial part of the last two decades. The second plot of Figure 2 shows the inflation target, which declines steadily from the early 1980s until the end of the 1990s and has been fluctuating around 2% since then. The third plot shows the risk premium variable w_t (eqs. 4 and 23). This variable is identified up to its sign, so that changing the signs of all

[14] While we assume a uniform measurement error standard deviation across maturities and time for nominal yields (σ_r), we allow two values for real real: σ_r outside low-liquidity periods, and $\sigma_r + \sigma_{r,liq}$ during 2008-2009 and before 2004, when TIPS were less liquid or unavailable, and during the COVID period, from March 2020 to February 2021. This flexibility allows the model to account for the illiquidity premium of up to 100 basis points during the great financial crisis and before 2004 as reported in D'Amico et al. (2018).

the components of $\boldsymbol{\lambda}_{1,w}$ and the signs of correlations of $\varepsilon_{w,t}$ with other shocks (i.e., $\sigma_{w,g}$, $\sigma_{w,z}$ and $\sigma_{w,\pi}$) results in a model with the exact same fit but with w_t of opposite sign. We choose identification scheme that results in a positive correlation between w_t and the nominal term premiums.

4.4. Term premiums

Since our model captures the joint dynamics of nominal and real yield curves, we can derive estimates of nominal, real, and inflation risk premiums using the following equations:

$$\begin{aligned} TPN_{t,h} &= -\frac{1}{h}(\log \mathbb{E}_t^{\mathbb{Q}}\left[\exp(-i_t - \cdots - i_{t+h-1})\right] - \\ &\qquad \log \mathbb{E}_t^{\mathbb{P}}\left[\exp(-i_t - \cdots - i_{t+h-1})\right]), \qquad (26) \\ TPR_{t,h} &= -\frac{1}{h}(\log \mathbb{E}_t^{\mathbb{Q}}\left[\exp(-i_t - \cdots - i_{t+h-1} + \pi_{t+1} + \ldots \pi_{t+h})\right] - \\ &\qquad \log \mathbb{E}_t^{\mathbb{P}}\left[\exp(-i_t - \cdots - i_{t+h-1} + \pi_{t+1} + \ldots \pi_{t+h})\right]), \qquad (27) \\ IRP_{t,h} &= -\frac{1}{h}\Big(\log \mathbb{E}_t^{\mathbb{Q}}\left[\exp(\pi_{t+1} + \ldots \pi_{t+h})\right] - \log \mathbb{E}_t^{\mathbb{P}}\left[\exp(\pi_{t+1} + \ldots \pi_{t+h})\right]\Big), \qquad (28) \end{aligned}$$

where $\mathbb{E}^{\mathbb{P}}$ denotes the expectation under the physical probability measure. These term premiums correspond to the components of nominal yields, real yields, and the break-even inflation rate, respectively, that would not exist if prices of risk $\boldsymbol{\lambda}_t$ were equal to zero.

Figure 3 displays the 10-year nominal, real, and inflation term premiums, together with estimates based on alternative strategies that have been proposed in the literature (namely Kim and Wright, 2005; Adrian et al., 2013; D'Amico et al., 2018). While the different estimates show similar low-frequency fluctuations, including a secular decrease in the nominal and real term premiums over the last fourty years, some differences are also apparent. In particular, since 2020, our estimates of the nominal (respectively real) term premiums are about 50 to 100 basis points higher than those obtained by Kim and Wright (2005) and Adrian et al. (2013) (resp. by D'Amico et al., 2018).

4.5. Impulse responses

Because the state vector follows a Gaussian VAR (Equation 3), the responses of macroeconomic variables to shocks are derived using standard VAR formulas. Figure 4, for example, displays the responses of inflation, the output gap, and the shadow rate to the various shocks

Figure 1: **Model fit of macroeconomic variables**. This figure shows the model fit of macroeconomic variables. Panel (a) shows the inflation rate (monthly growth rate of the price index, annualized), and the $\bar{\pi}_t$ and π_t^* components of inflation (see eq. 20). Panel (b) compares the model-implied target rate π_t^* with the Perceived Target Rate of Brayton et al. (2014), that is used in the estimation. Panel (c) shows the trend growth rate g_t, together with the monthly GDP growth rate based on the approach proposed by Brave et al. (2019). Panel (d) displays the model-implied output gap, together with that extracted from the FRED database (calculated as $\log(GDPC1/GDPPOT)$). All rates are annualized and expressed in percent.

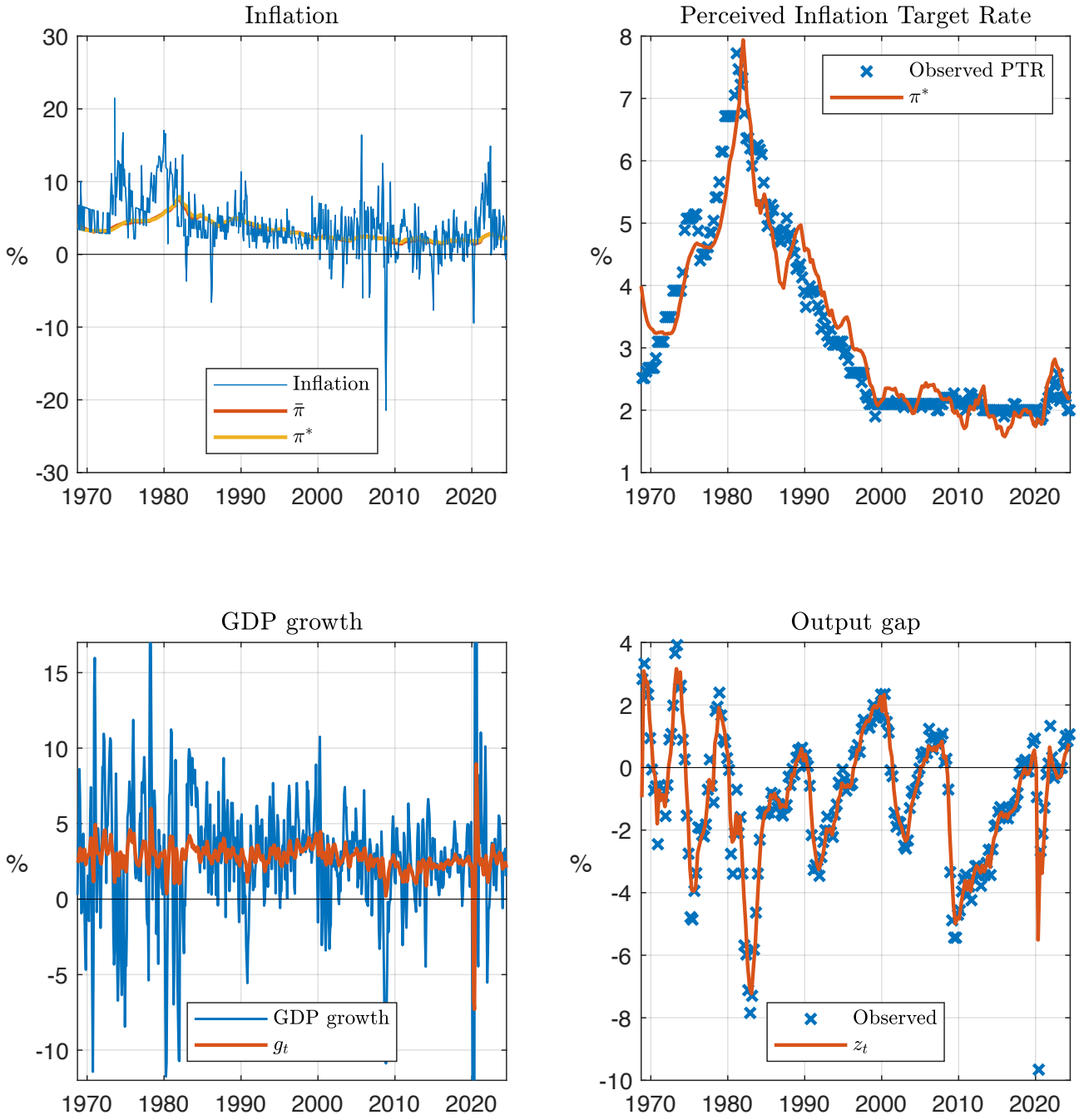

Figure 2: **Natural rate of interest (r^*) and inflation target (π^*).** This figure shows the estimated natural rate of interest (r_t^* in eq. 16), and compares it with the estimates of Laubach and Williams (2003) and Holston et al. (2017). The second plot shows the inflation target (π_t^* in eq. 18). The third plot shows the time series of the risk premium factor w_t (eq. 24), that drives the prices of risk (eq. 23). The grey area corresponds to the 95% confidence interval (reflecting filtering uncertainty).

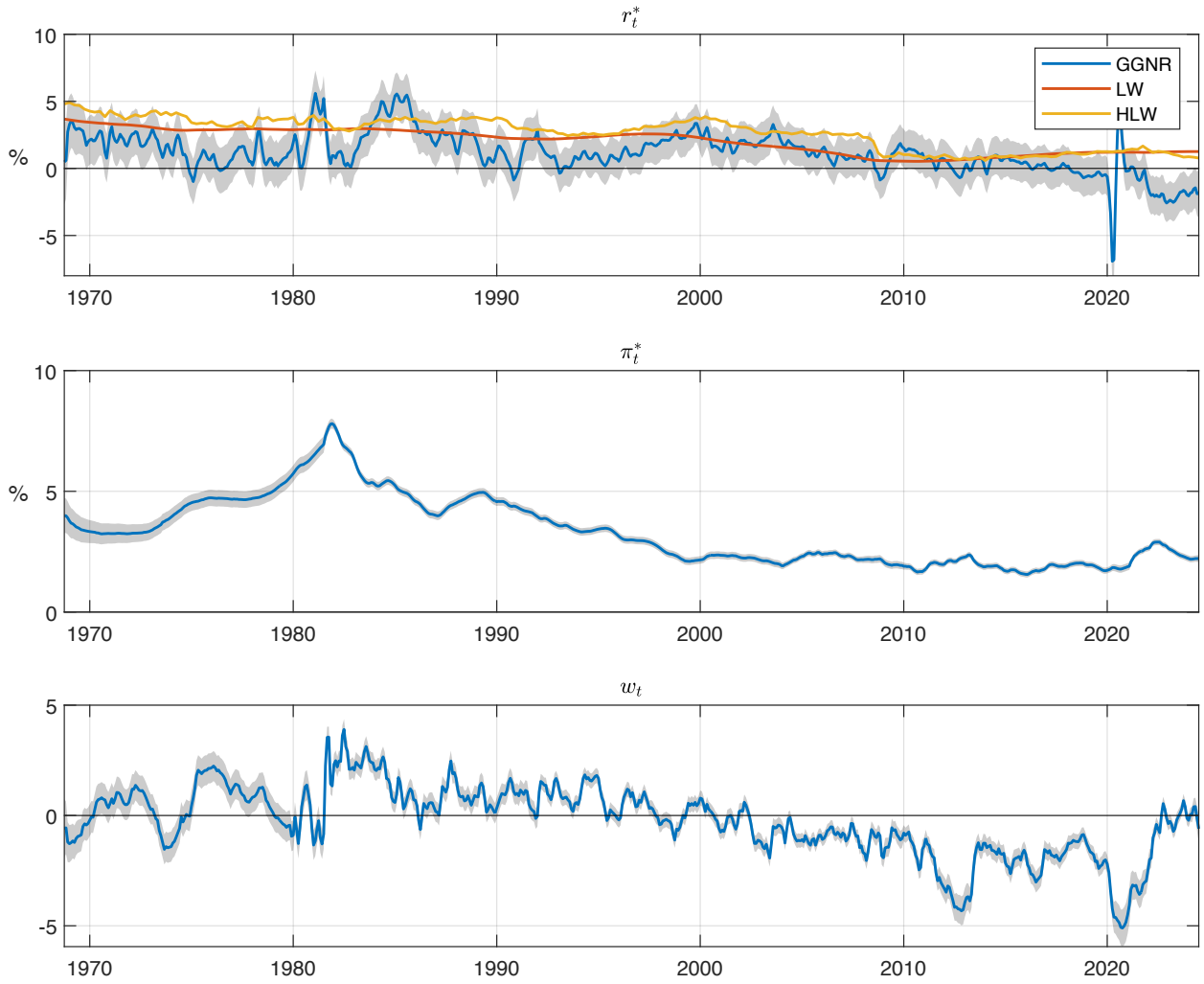

Figure 3: **Term premium estimates**. This figure shows model-implied term premiums, together with alternative estimates based on Kim and Wright (2005), Adrian et al. (2013), D'Amico et al. (2018). Term premiums are expressed in percent (annualized). Formal definitions of the nominal, real, and inflation term premiums are respectively given in (26), (27), and (28). The inflation risk premium is defined as the difference between the nominal and the real term premium. Model-free risk premiums are based on observed yields and survey only; for instance, the model-free inflation risk premium is calculated by subtracting the survey-based inflation forecast to the break-even inflation rate (calculated as the difference between the nominal yield and the real yield). Shaded areas indicate NBER recessions.

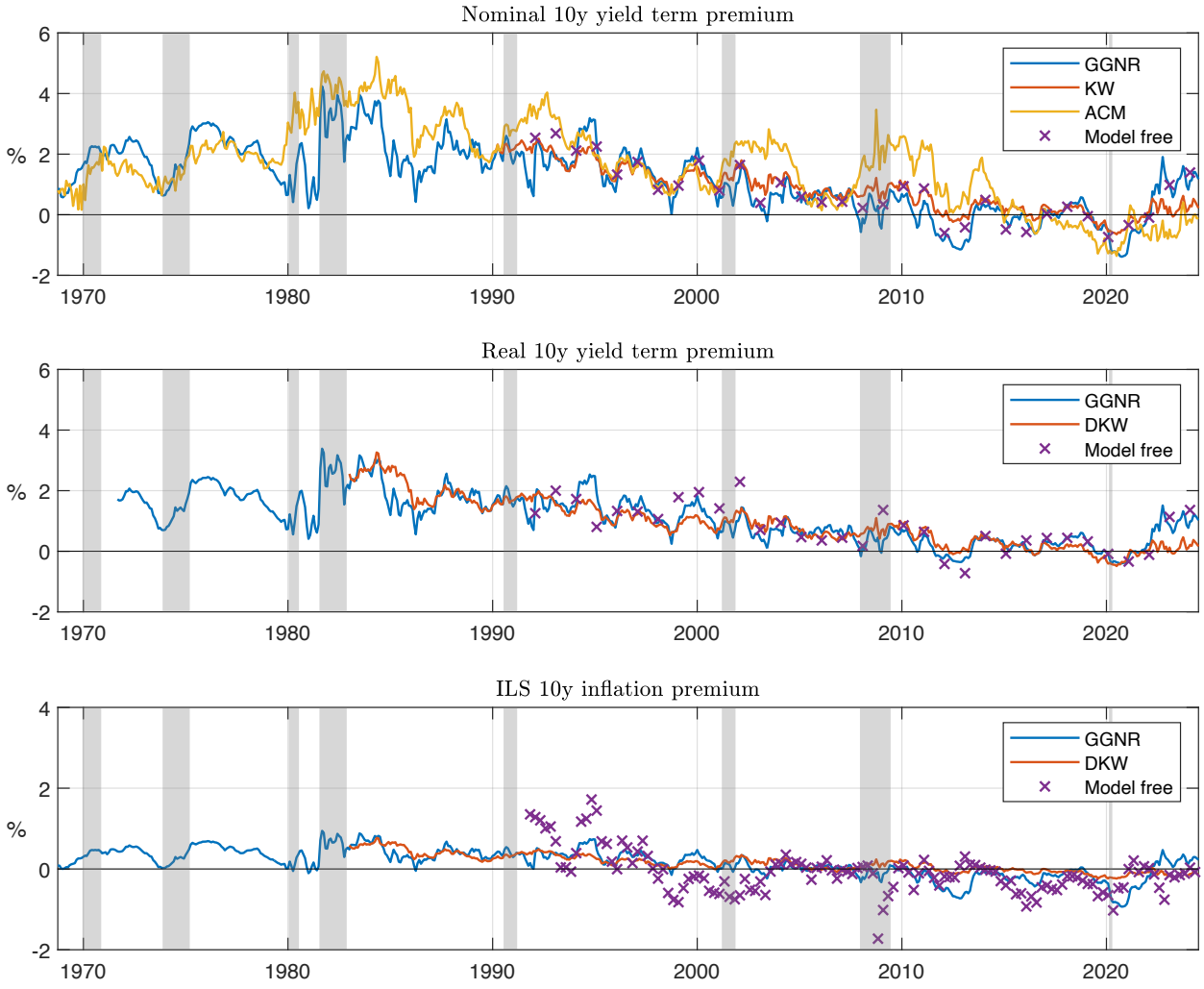

included in the model. These responses exhibit the expected signs, given the model's structure. The first row shows the response to a tightening monetary policy shock ($\varepsilon_{i,t}$ in eq. 14); the desinflationary and recessionary effects peak at approximately 2.5 years.

Let us now turn to the responses of long-term real and nominal yields. These responses cannot be obtained with standard techniques since yields—nominal and real—are nonlinear functions of the state vector $\mathbf{x}_t$. The impulse response of different yields will depend, in particular, on the level of the shadow rate. Intuitively, when the shadow rate is negative, the impact of (any type of) shocks on yields are expected to be muted, consistently with the lower yield volatility observed during ZLB periods. To fix ideas, consider the effect of an increase in $\varepsilon_{i,t}$ by 25 bps (annualized). The effect of this shock on the shadow rate does not depend on the level of s_t since the latter is part of $\mathbf{x}_t$, that itself follows a homoskedastic VAR model. (This response is shown in the last column of plots of Figure 4.) However, the impact of this shock on $i_t = \max(0, s_t)$ depends on s_t. For instance, if s_t is equal to -1% (annualized), then i_t is not affected by this shock upon impact. If the shadow rate is persistent, this amortization effect persists for the next few periods (in expectation). Indeed, if the shadow rate is persistent and if $s_t = -1\%$, then it is likely that s_t will stay negative for the next few periods, even if it is augmented by 0.25% today. Accordingly, the 0.25% shock on s_t will have a smaller effect on expected future short-term rates (i_t) when $s_t = -1\%$ than when $s_t > 0\%$. Since long-term rates can be approximated by averages of expected future short-term rates (i_t), this effect is transmitted to interest rates of longer maturity.

To quantitatively investigate these effects in our framework, we compute non-linear impulse response functions in the spirit of Potter (2000). Consider a function q of $\mathbf{x}_t$. In our context, $q(\mathbf{x}_t)$ can be, for instance, a nominal or a real long-term yield. we define the general conditional impulse response function as:

$$\begin{aligned} IRF_h(q, \mathbf{\Gamma}, \mathbf{b}, \mathbf{d}) &= \mathbb{E}(q(\mathbf{x}_{t+h})|\mathbf{\Gamma}\mathbf{x}_{t-1} = \mathbf{b}, \boldsymbol{\varepsilon}_t = \mathbf{d}) - \\ &\quad \mathbb{E}(q(\mathbf{x}_{t+h})|\mathbf{\Gamma}\mathbf{x}_{t-1} = \mathbf{b}, \boldsymbol{\varepsilon}_t = \mathbf{0}), \end{aligned} \tag{29}$$

where matrix $\mathbf{\Gamma}$ determines the linear combinations of $\mathbf{x}_t$ that serve as conditioning information, and $\mathbf{d}$ determines the shock that one wants to apply to the system on date t. To fix ideas, assume we consider the yield curve response to a monetary-policy shock ($\varepsilon_{i,t}$) in the context

Figure 4: **Impulse response functions of inflation, output gap, and the shadow rate**. This figure shows the impulse response functions of inflation (or more precisely of its persistent component, $\bar{\pi}_t$) and of the output gap to different shocks (one standard deviation for each shock). $\varepsilon_{i,t}$ is a monetary policy shock (eq. 14); $\varepsilon_{g,t}$ is a shock to the trend growth rate (eq. 19); $\varepsilon_{z,t}$ is a demand shock (eq. 15); ε_t^* is an inflation target shock (eq. 18); $\varepsilon_{\pi,t}$ is an inflation shock (eq. 21). The first column shows inflation responses (expressed in percentage points, annualized). The second column shows output gap responses (expressed in percentage points). The third column shows shadow rate responses (expressed in percentage points). The x-axis indicates to the number of months after the shock.

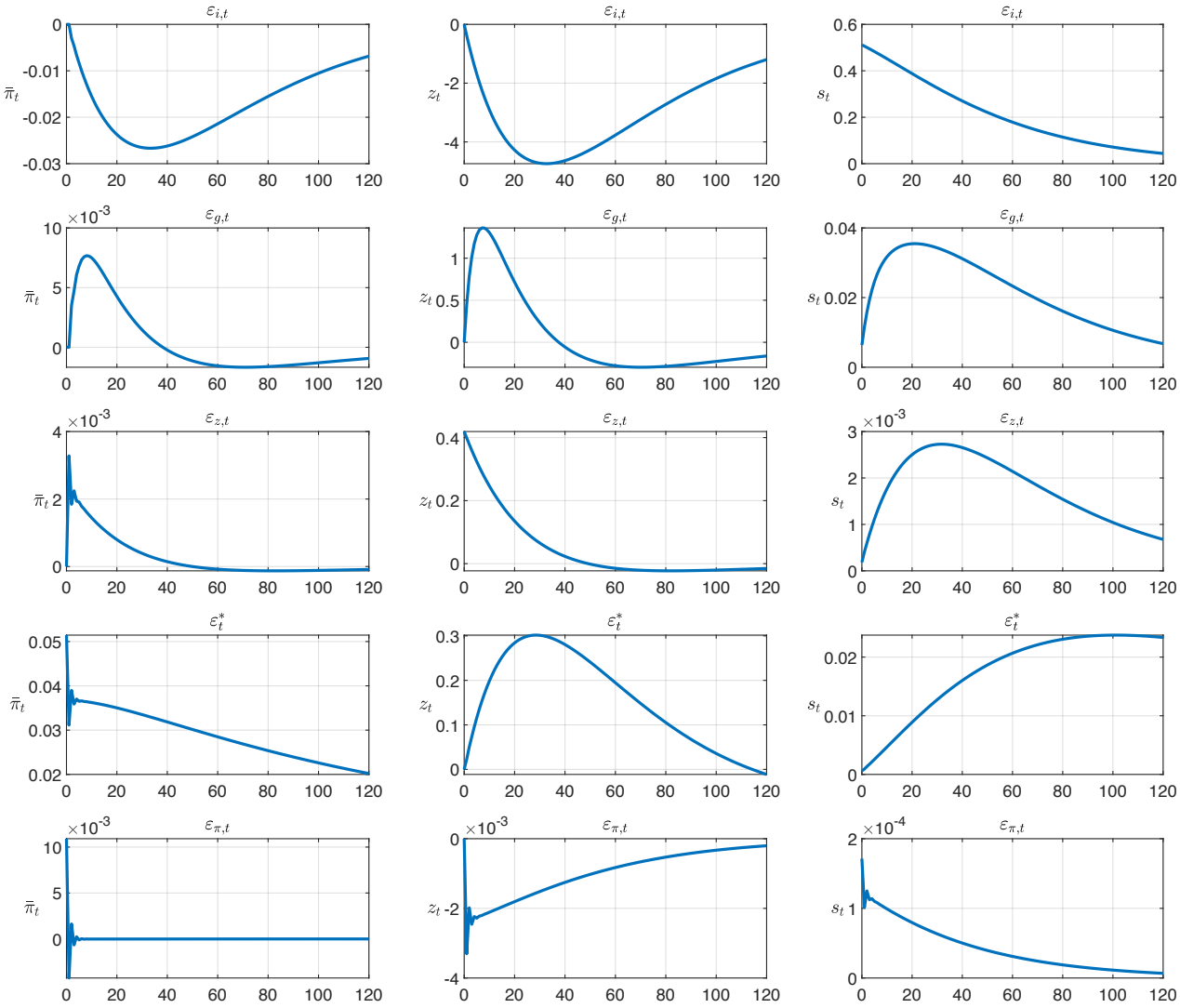

Figure 5: **Responses of yields to monetary policy shocks ($\varepsilon_{i,t}$), conditional on** s. This figure shows the impulse response functions of nominal and real yields to an accommodative monetary policy shock (increase in the shadow rate by 25 basis points, via $\varepsilon_{i,t}$, see eq. 14) conditional on the initial value of the shadow rate (s_t). It shows that yields are less responsive in the lower bound regime.

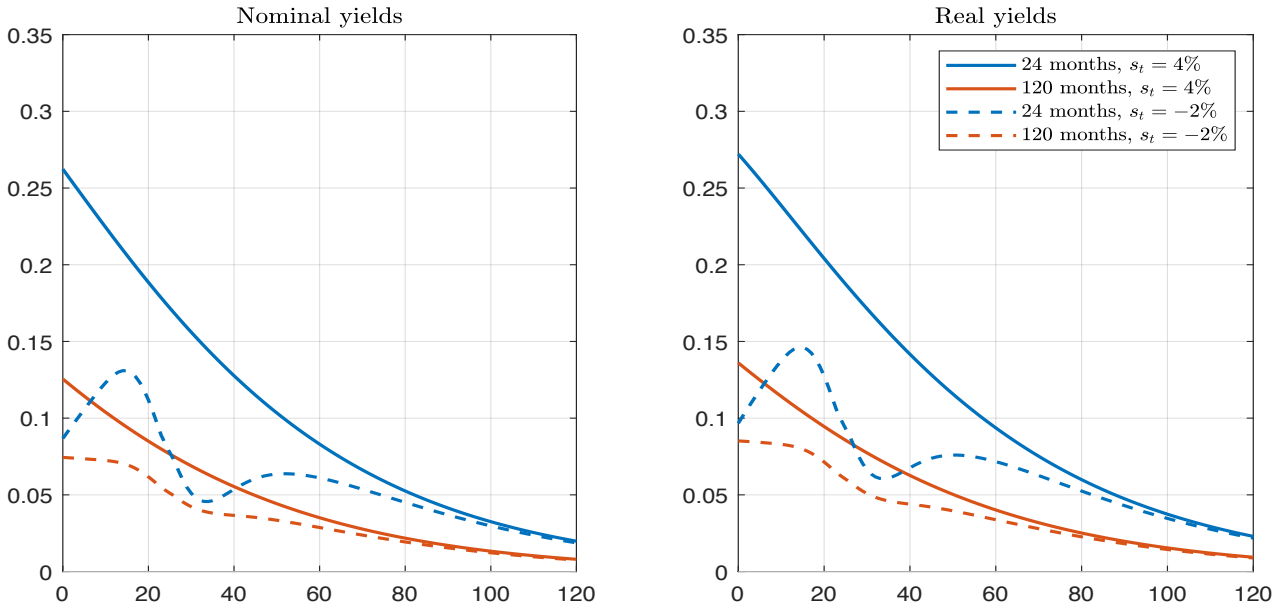

Figure 6: **Responses of yields to monetary policy shocks ($\varepsilon_{i,t}$), conditional on** $r^* + \pi^*$. This figure shows the impulse response functions of nominal and real yields to a tightening monetary policy shock (increase in the shadow rate by 25 basis points, via $\varepsilon_{i,t}$, see eq. 14) when we are initially close to the zero-lower bound ($i_t = s_t = 0\%$), conditional on the initial value of the equilibrium nominal rate ($r_t^* + \pi_t^*$). It shows that yields are slightly less responsive when $r_t^* + \pi_t^*$ is low.

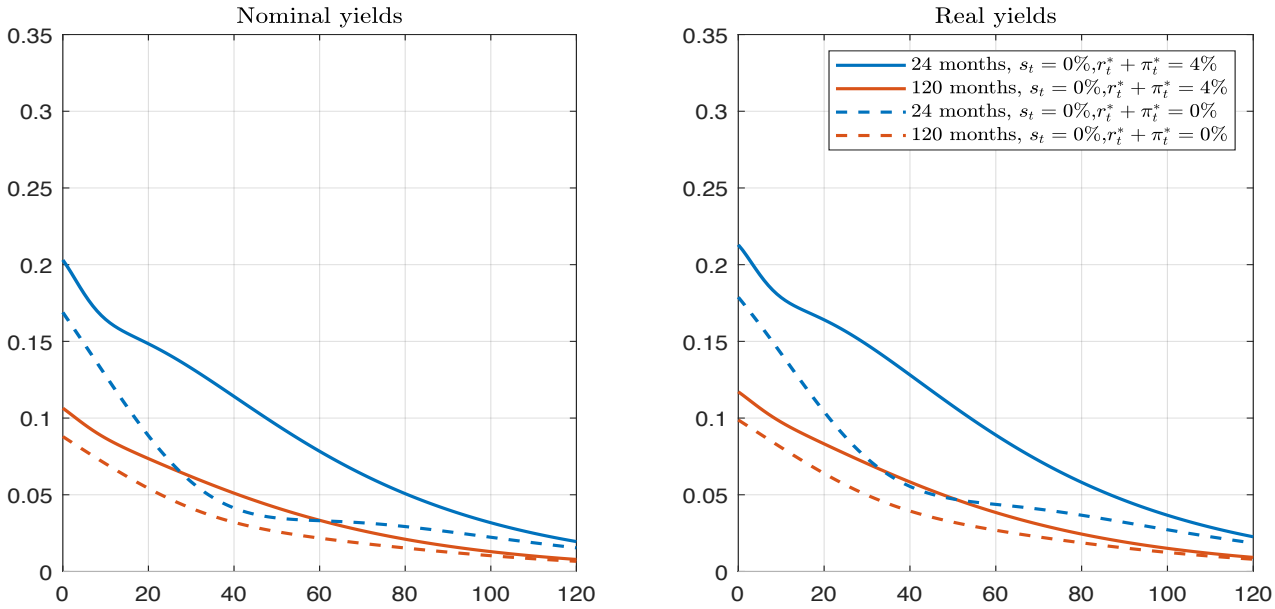

of a specific value of the shadow rate, say $s_{t-1} = \bar{s}$. In that case, we have:

$$\mathbf{\Gamma} = \begin{bmatrix} 1 & 0 & \dots \end{bmatrix}, \quad \mathbf{b} = \begin{bmatrix} \bar{s} \end{bmatrix}, \quad \text{and} \quad \mathbf{d} = \begin{bmatrix} \frac{0.25\%\Delta t}{\sigma_i} & 0 & \dots \end{bmatrix}', \tag{30}$$

where Δt is the length of a model period expressed as a fraction of a year.

Appendix C details an approximate second-order calculation of eq. (29) in the context of our framework. This computation makes, in particular, use of the fact that the conditional distribution $\mathbf{x}_{t+h}|\{\mathbf{\Gamma}\mathbf{x}_{t-1} = \mathbf{b}, \boldsymbol{\varepsilon}_t = \mathbf{d}\}$, appearing in eq. (29), is available in closed form.[15]

Figure 5 displays impulse response functions (IRFs) of nominal and real yields to a 0.25% (annualized) shock to $\varepsilon_{i,t}$ under two scenarios: a non-binding ZLB ($s_t = 4\%$, solid lines) and a binding ZLB ($s_t = -2\%$, dashed lines). As expected, the IRFs indicate a more muted response of yields when the ZLB binds, especially at shorter maturities (e.g., the 2-year yield is more affected than the 10-year yield). This is because short-term yields face greater constraints at the ZLB due to a larger expected fraction of their time before maturity being constrained by the ZLB. The right panel of Figure 5 shows the responses of real yields to the same shock. We find that the reaction of real yields is also dampened when conditioning on a negative value of s_t. Notice that while Figure 5 shows the impact of monetary policy shocks ($\varepsilon_{i,t}$) on yields, this dampening effect is also observed for other shocks, illustrating the overall reduction in yield volatility during ZLB periods.

While shocks to $\varepsilon_{i,t}$ represent monetary policy shocks as they enter the model via the central bank's reaction function (eq. 14), it is important to note that these shocks do not translate into changes in the policy rate—i.e., the one-period rate of the model—when the shadow rate (s_t) is negative, which then makes their quantitative interpretation unclear. We therefore conduct an additional analysis focusing solely on scenarios with $s_t \geq 0$, ensuring that shocks to $\varepsilon_{i,t}$ fully transmit to the nominal short-term rate i_t. Interestingly, while the amortization effect is much smaller when $s_t \geq 0$, a small effect can subsist when s_t is positive but close to zero, especially in conditions favoring future ZLB periods. Figure 6 shows, for instance, that when conditioning on $s_t = 0\%$, the yield response to a 25-basis-point increase in $\varepsilon_{i,t}$ is smaller when

[15] Specifically, this conditional distribution is multivariate Gaussian, owing to the closure of the multivariate normal under linear transformations and conditioning.

the initial equilibrium nominal short-term rate, $i_t^* = r_t^* + \pi_t^*$, is low.[16] This is because low r_t^* increases the probability of future ZLB events, and the occurrence of these events tends to dampen the impact of the shock on yields. To better understand, consider an extreme case where $r_t^* = -10\%$. Even with $s_t = 0$, s_t is then likely to become negative shortly thereafter, and i_t will then hit zero, regardless of the 25-basis-point increase; this will therefore result in a muted response of the yields to the shock. Conversely, if $r_t^* = 10\%$, the probability of a binding ZLB in subsequent periods is low, leading to the full transmission of the monetary policy shock.

4.6. Conditional frequency of ZLB periods

Our framework can be exploited to investigate how specific environments influence the frequency of ZLB regimes. Several researchers have highlighted, for instance, that the frequency of ZLB episodes may depend on the level of the natural rate of interest or the inflation target (e.g., Chung et al., 2012; Bianchi et al., 2021; Fernández-Villaverde et al., 2023).

Assume that we want to compute the frequency of hitting the ZLB conditional on $r_t^* = x$ and $\pi_t^* = y$, say. This frequency is equal to

$$\mathbb{P}\left(s_t < \underline{i} | r_t^* = x, \pi_t^* = y\right).$$

The distribution of s_t, conditionally on $\{r_t^* = x, \pi_t^* = y\}$, is Gaussian. Hence, we have:[17]

$$\mathbb{P}\left(s_t < \underline{i} | r_t^* = x, \pi_t^* = y\right) = \Phi^{\mathcal{N}}\left(\frac{\underline{i} - e(x,y)}{\sqrt{v}}\right),$$

where $e(x,y) := \mathbb{E}(s_t | r_t^* = x, \pi_t^* = y)$ and $v := \mathbb{V}ar(s_t | r_t^* = x, \pi_t^* = y)$.

Figure 7 uses the previous formulas to illustrate how the probability of hitting the ZLB depends on the natural interest rate (r_t^*) and the inflation target (π_t^*). The iso-probability curves in the figure appear to be close to lines relating constant sums of r_t^* and π_t^* (i.e., con-

[16] Supplemental Appendix V presents additional analyses. Figure E.12 displays IRFs conditioning only on r_t^* (and not on $i_t^* = r_t^* + \pi_t^*$), while Figure E.13 examines the impact of a negative 0.25% monetary policy shock on s_t (from 0.25% to 0%).

[17] Since

$$\begin{bmatrix} \mathbf{\Gamma} \mathbf{x}_t \\ \delta_0 + \delta_1' \mathbf{x}_t \end{bmatrix} \sim \mathcal{N}\left(\begin{bmatrix} \mathbf{\Gamma} \mathbf{e}_X \\ \delta_0 + \delta_1' \mathbf{e}_X \end{bmatrix}, \begin{bmatrix} \mathbf{\Gamma} \mathbf{V}_X \mathbf{\Gamma}' & \mathbf{\Gamma} \mathbf{V}_X \delta_1' \\ \delta_1' \mathbf{V}_X \mathbf{\Gamma}' & \delta_1' \mathbf{V}_X \delta_1 \end{bmatrix}\right),$$

it comes that: $e(x,y) = \delta_0 + \delta_1' \mathbf{e}_X + \delta_1'(\mathbf{V}_X \mathbf{\Gamma}')(\mathbf{\Gamma} \mathbf{V}_X \mathbf{\Gamma}')^{-1}(\mathbf{b} - \mathbf{\Gamma} \mathbf{e}_X)$ and $v(x,y) = \delta_1' \mathbf{V}_X \delta_1 - \delta_1'(\mathbf{V}_X \mathbf{\Gamma}')(\mathbf{\Gamma} \mathbf{V}_X \mathbf{\Gamma}')^{-1}(\mathbf{V}_X \mathbf{\Gamma}')' \delta_1$, where $\mathbf{\Gamma}$ is such that $\mathbf{\Gamma} \mathbf{x}_t = [r_t^*, \pi_t^*]'$ and $\mathbf{b} = [x, y]'$. Note that v does not depend on x and y.

stant equilibrium nominal short-term rate, see Bauer and Rudebusch, 2020). In other words, combinations of r_t^* and π_t^* that yield the same i_t^* result in similar ZLB probabilities. The figure demonstrates a substantial increase in ZLB probability as the equilibrium nominal rate decreases; for instance, it rises from 5% at $i_t^* = 4\%$ to 10% at $i_t^* = 2.5\%$.[18]

4.7. The Mundell-Tobin effect

Shadow-rate models are well-known to effectively capture the volatility compression that occurs at the ZLB (e.g., Christensen and Rudebusch, 2015). Because our shadow-rate model features real and nominal yields, we can use it to explore the effects of ZLB on other conditional moments relating yields and macroeconomic variables. In particular, we can analyse how ZLB affects the change in the conditional correlation between real rates and inflation. This correlation is at the heart of the so-called Mundell-Tobin effect (Mundell, 1963; Tobin, 1965; Fama and Gibbons, 1982), according to which increases in inflation are associated with higher nominal interest rates, but lower real interest rates, driving a negative correlation between expected inflation and real rates.

One can compute this correlation in any model featuring real rates and inflation. In Gaussian affine term structure models involving real and nominal yield curves (e.g., Hördahl et al., 2006; Rudebusch and Wu, 2008; Chernov and Mueller, 2012), this correlation would be constant as these models are homoskedastic. Using a regime-switching term structure model of interest rates, Ang et al. (2008) compute this conditional correlation in different regimes and find weak evidence for the Mundell-Tobin effect, in the sense that the correlation is negative in only a fraction of the regimes they identify.

Figure 8 displays the model-implied 12-month-ahead conditional correlations between real rates of different maturities and expected inflation over the same maturity. The correlations are negative, consistently with the Mundell-Tobin effect. While these correlations remain relatively constant and negative during the pre-ZLB era—reflecting the GATSM-like behavior of the model when the short-term rate is far from the ZLB—they vary and become significantly more negative during ZLB periods. This enhanced effect stems from the fact

[18] This figure illustrates in particular that the influence of r^* and π^* on this probability is nearly symmetric. This might seem unexpected considering that r^* and π^* do not enter the Taylor rule (equation 14) in a symmetric manner. However, this arises because π_t fluctuates locally around its trend π_t^*, which makes the term $\pi_t - \pi_t^*$ in the Taylor rule relatively insensitive to the value of π_t^*.

that, during ZLB periods, nominal interest rates are constrained and therefore move less than expected inflation, thus amplifying the negative correlation between real rates and expected inflation.

5. Conclusion

This paper advances the literature on shadow-rate models by incorporating real interest rates, providing a comprehensive framework for analyzing yield curve dynamics, particularly during periods of zero lower bound (ZLB). The model, applied to US data spanning five decades, delivers novel estimates of real and nominal term premiums and reveals how shocks differentially impact real and nominal yields under ZLB constraints. The analysis empirically confirms the Mundell-Tobin effect, demonstrating its intensification during ZLB periods due to constraints on nominal interest rates. Furthermore, the model quantifies the significant increase in ZLB probability as the equilibrium nominal interest rate falls, offering a new perspective on the relationship between monetary policy and the likelihood of ZLB events.

Figure 7: **Conditional probabilities or being in the lower-bound regime**. This figure illustrates the influence of the natural rate of interest (r^*) and of the inflation target (π^*) on the frequency of lower-bound regimes. Specifically, the blue curves show combinations of r^* and π^* that yield a given conditional probability (labeled on each curve) of being in the lower-bound regime.

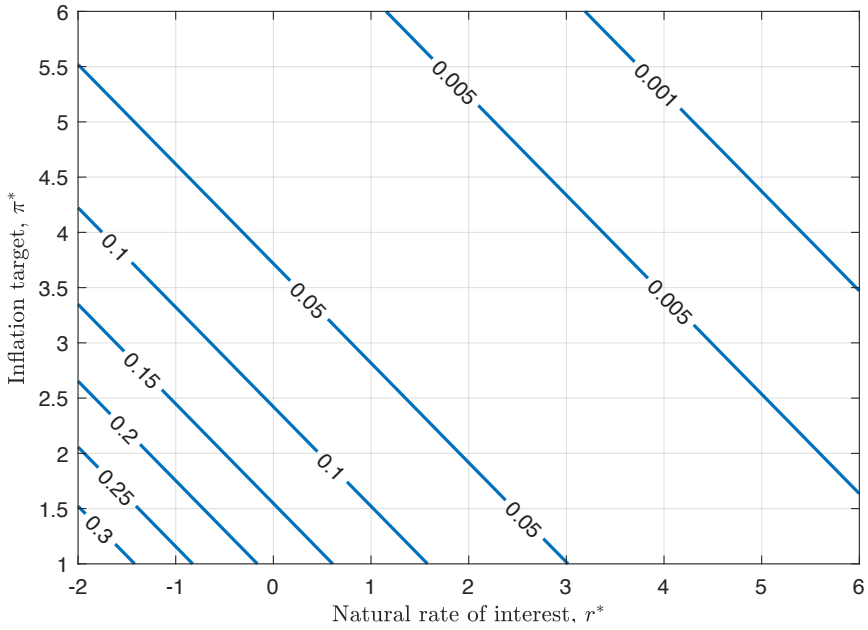

Figure 8: **Conditional correlation between real rates and expected inflation**. This figure shows 12-month-ahead conditional correlations between real rates and expected inflation with maturities 3 month, 12 months and 120 months. Specifically, it shows $\mathbb{C}orr_t(r_{t+12,h}, \mathbb{E}_{t+12}(\bar{\pi}_{t+12+h}))$.

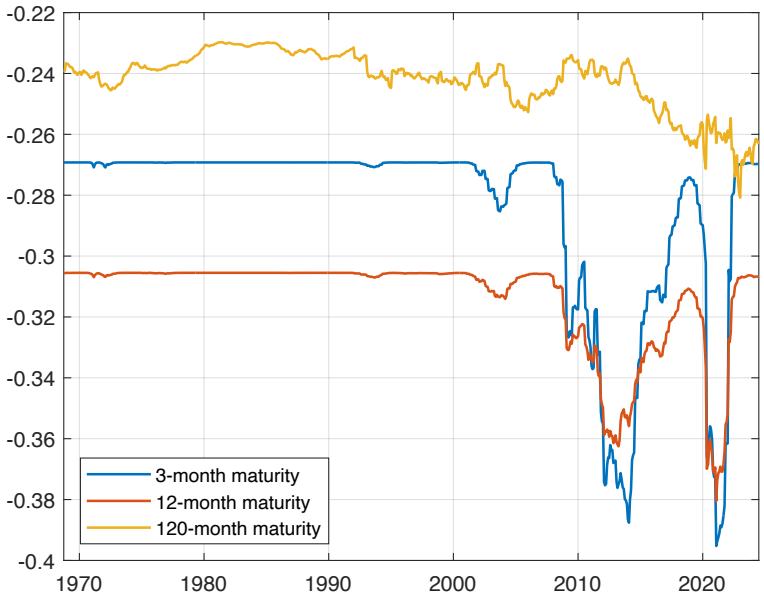

Appendix A. Extension of Wu and Xia (2016)

Lemma 1. *Consider a process* $\mathbf{x}_t$ *following a Gaussian vector autoregressive process:*

$$\mathbf{x}_t = \boldsymbol{\mu} + \boldsymbol{\Phi}\mathbf{x}_{t-1} + \boldsymbol{\Sigma}\boldsymbol{\varepsilon}_t, \quad \boldsymbol{\varepsilon}_t \sim \ i.i.d. \mathcal{N}(\mathbf{0}, \boldsymbol{I}).$$

If $\mathbf{b}'\mathbf{x}_t$ *is a persistent process, the following conditional expectation:*

$$\begin{aligned} K_h(\mathbf{x}_t, a, \mathbf{b}, \mathbf{c}) \quad = \quad & \mathbb{E}_t(\exp[-\max(\underline{i}, a + \mathbf{b}'\mathbf{x}_{t+1}) - \cdots - \max(\underline{i}, a + \mathbf{b}'\mathbf{x}_{t+h}) \\ & + \mathbf{c}'\mathbf{x}_{t+1} + \cdots + \mathbf{c}'\mathbf{x}_{t+h}]) \end{aligned}$$

can be approximated with

$$\exp(-F_{0,1,t} - \cdots - F_{h-1,h,t}),$$

where

$$F_{n-1,n,t} \quad = \quad \underline{i} + \sigma_n g\left(\frac{a_n + \mathbf{b}_n'\mathbf{x}_t - \underline{i}}{\sigma_n}\right) - (\dot{c}_n + \mathbf{c}_n'\mathbf{x}_t) + \Phi^{\mathcal{N}}\left(\frac{\bar{a}_n + \mathbf{b}_n'\mathbf{x}_t - \underline{i}}{\sigma_n}\right)\mathbf{b}'\boldsymbol{\Phi}_n\boldsymbol{\Sigma}\boldsymbol{\Sigma}'\boldsymbol{\Phi}_n'\mathbf{c}.$$

where

$$g(x) = x\Phi^{\mathcal{N}}(x) + \phi^{\mathcal{N}}(x),$$

$\Phi^{\mathcal{N}}$ *and* $\phi^{\mathcal{N}}$ *being the c.d.f. and the p.d.f. of the standard normal distribution, respectively. The* $\boldsymbol{\Phi}_n$ *matrices are defined as follows:*

$$\boldsymbol{\Phi}_0 = \mathbf{0}, \quad \textit{and} \quad \boldsymbol{\Phi}_n = \sum_{i=0}^{n-1} \boldsymbol{\Phi}^i \textit{ for } n > 0.$$

Moreover:

- $\mathbf{b}_n$, $\bar{a}_n$, a_n, *and* σ_n *are obtained as follows:*

$$\left\{\begin{array}{lcl} \mathbf{b}_n & = & (\boldsymbol{\Phi}^n)'\mathbf{b} \\ \bar{a}_n & = & a + \mathbf{b}'\boldsymbol{\Phi}_n\boldsymbol{\mu} \\ a_n & = & \bar{a}_n - \frac{1}{2}\mathbf{b}'\boldsymbol{\Phi}_n\boldsymbol{\Sigma}\boldsymbol{\Sigma}'\boldsymbol{\Phi}_n'\mathbf{b} \\ \sigma_n^2 & = & \sigma_{n-1}^2 + \mathbf{b}'\boldsymbol{\Phi}^{n-1}\boldsymbol{\Sigma}\boldsymbol{\Sigma}'\boldsymbol{\Phi}^{n-1\prime}\mathbf{b} \quad \textit{with } \sigma_0 = 0. \end{array}\right. \tag{A.1}$$

  (Note that $\bar{a}_n + \mathbf{b}_n'\mathbf{x}_t = \mathbb{E}_t(a + \mathbf{b}'\mathbf{x}_{t+n})$ *and* $\mathbb{V}ar_t(a + \mathbf{b}'\mathbf{x}_{t+n}) = \sigma_n^2$*.)*

- $\dot{c}_n$ *and* $\mathbf{c}_n$ *are obtained as follows:*

$$\left\{\begin{array}{lcl} \dot{c}_n & = & \mathbf{c}'\boldsymbol{\Phi}_n\boldsymbol{\mu} + \frac{1}{2}\mathbf{c}'\boldsymbol{\Phi}_n\boldsymbol{\Sigma}\boldsymbol{\Sigma}'\boldsymbol{\Phi}_n'\mathbf{c} \\ \mathbf{c}_n & = & (\boldsymbol{\Phi}^n)'\mathbf{c}, \end{array}\right. \tag{A.2}$$

  (Note that $\dot{c}_n + \mathbf{c}_n'\mathbf{x}_t = \mathbb{E}_t(\mathbf{c}'\mathbf{x}_{t+n}) + \frac{1}{2}\mathbf{c}'\boldsymbol{\Phi}_n\boldsymbol{\Sigma}\boldsymbol{\Sigma}'\boldsymbol{\Phi}_n\mathbf{c}$*.)*

Proof. See Online Appendix I. □

Appendix B. Parameter constraints

For identification purposes, as well as to facilitate the estimation and to achieve a satisfying relative fit of the different variables, we impose a number of constraints on the parameter space.

First, for macroeconomic variables, we require that the standard deviation of the measurement errors of the output gap (σ_o) is less than 0.5%, which we find to be a binding constraint. We relate the standard deviations of the (monthly) measurement errors for GDP growth and inflation to σ_o by setting $\sigma_{gdp} = \sigma_{inf} = \sigma_o/100$. For nominal rates, we assume a uniform standard deviation of measurement errors across all maturities, denoted as σ_n. For real rates, we apply two different values for the standard deviations of measurement errors over time to account for the relatively lower reliability of our data during three periods when TIPS were either less liquid or nonexistent: (i) prior to 2004, (ii) during the global financial crisis (2008-2009) (see D'Amico et al., 2018) and (iii) during the COVID crisis (March 2020 - February 2021). Specifically, outside of these periods, we estimate the standard deviation or real rates for all maturities as σ_r, and during the low liquidity episodes, the standard deviation of measurement errors is estimated as $\sigma_r + \sigma_{r,liq}$. We assume that the standard deviation of measurement errors for the perceived target rate (σ_{ptr}) is larger than that of inflation surveys (σ_s); specifically $\sigma_{ptr} = 5\sigma_s$. (For the surveys, this uniform standard deviation applies to both horizons we consider.) Regarding the measurement errors associated with surveys on the 3-month T-bill rate, to ensure that the term premium generated by the model aligns with market expectations, we set their standard deviation to a quarter of the value used for the other surveys, i.e., $\sigma_t = \sigma_s/4$.

To assure numerical stability of the system, we impose the upper bound of 0.995 on the autoregressive persistence parameters.[19] We found that this constraint is binding for ρ_κ, the autoregressive parameter of the pure preference for present (eq. 17), and ρ^*, the autoregressive parameter of the inflation target (eq. 18).

We restrict the conditional standard deviation of monthly r^* to 0.0056, the value reported in Laubach and Williams (2003).[20] We also restrict the unconditional mean of κ_t (eq. 17) to be non-negative, i.e., $\mu_\kappa \geq 0$.

To facilitate the estimation of α and β, we impose that the contribution of monetary policy shocks to the variance of the one-year-ahead inflation ($\bar{\pi}_t$) forecast error is not smaller than

[19] In particular, this implies that we constrain the natural rate of interest r_t^* and the inflation target π_t^* to be stationary (contrary to, e.g. Laubach and Williams, 2003; Holston et al., 2017, for r_t^*). Imposing these variables to be stationary is consistent with the existence of a finite variance for these objects. Recent research by Rogoff et al. (2024) provides strong and consistent evidence of trend stationarity in long-horizon series of the real short-term rate, suggesting the stationary nature of the natural rate of interest. Studies imposing a stationary natural rate of interest include, e.g., Mésonnier and Renne (2007) and Fries et al. (2018).

[20] In practice, this is implemented by setting $\sigma_\kappa = \sqrt{0.0056^2 - \sigma_g^2}$ (subject to $\sigma_g < 0.0056$).

5%, which is broadly in line with the empirical evidence: Uhlig and Amir-Ahmadi (2012) find that this share is of 25%, Uhlig (2005) finds approximately 15%, Herwartz et al. (2022) find 5%, Gorodnichenko and Lee (2017) find about 10%. In estimation we find that the 5% restriction is binding. Besides, we use the standard values of 1.5 and 0.5 for α_π and α_z in the Taylor rule (eq. 14).[21]

We assume that $\varepsilon_{i,t}$, $\varepsilon_{g,t}$, $\varepsilon_{z,t}$, ε^*_t, and $\varepsilon_{i,\pi}$ are priced, in the sense that SDF innovations correlate to these shocks. This implies that five entries of $\boldsymbol{\lambda}_0$ and $\boldsymbol{\lambda}_{1,w}$ (appearing in eq. 23) are nonzero. Since w_t is unobserved, for identification purposes, we set its mean to zero ($\mu_w = 0$) and we impose $\sigma_w = \sqrt{1-\rho_w^2}$, so that its unconditional variance would be equal to 1 if it were uncorrelated with other variables (i.e., if $\sigma_{w,z} = \sigma_{w,g} = \sigma_{w,\pi} = 0$).

Finally, we set $\underline{i} = 0$, $\theta = 1$, and μ_g and μ^* are set equal to the sample means of GDP growth and inflation, respectively.

Appendix C. Conditional non-linear impulse response functions

Consider a function q of $\mathbf{x}_t$. In the spirit of Potter (2000), we define the conditional impulse response function as:

$$IRF_h(q, \boldsymbol{\Gamma}, \mathbf{b}, \mathbf{d}) = \mathbb{E}(q(\mathbf{x}_{t+h})|\boldsymbol{\Gamma}\mathbf{x}_{t-1} = \mathbf{b}, \boldsymbol{\varepsilon}_t = \mathbf{d}) - \mathbb{E}(q(\mathbf{x}_{t+h})|\boldsymbol{\Gamma}\mathbf{x}_{t-1} = \mathbf{b}, \boldsymbol{\varepsilon}_t = \mathbf{0})$$

In the present framework,

$$\mathbf{x}_t \sim \mathcal{N}(\mathbf{e}_X, \mathbf{V}_X),$$

where

$$\mathbf{e}_X = (\boldsymbol{I}_{n\times n} - \boldsymbol{\Phi})^{-1}\boldsymbol{\mu}, \quad \text{and} \quad \text{vec}(\mathbf{V}_X) = (\boldsymbol{I}_{n^2\times n^2} - \boldsymbol{\Phi}\otimes\boldsymbol{\Phi})^{-1}\,\text{vec}(\boldsymbol{\Sigma}\boldsymbol{\Sigma}').$$

Moreover, we have:

$$\begin{bmatrix} \boldsymbol{\varepsilon}_t \\ \boldsymbol{\Gamma}\mathbf{x}_{t-1} \\ \mathbf{x}_{t+h} \end{bmatrix} \sim \mathcal{N}\left(\begin{bmatrix} \mathbf{0} \\ \boldsymbol{\Gamma}\mathbf{e}_X \\ \mathbf{e}_X \end{bmatrix}, \begin{bmatrix} \boldsymbol{I} & \mathbf{0} & \boldsymbol{\Sigma}'\boldsymbol{\Phi}^{h'} \\ \mathbf{0} & \boldsymbol{\Gamma}\mathbf{V}_X\boldsymbol{\Gamma}' & \boldsymbol{\Gamma}\mathbf{V}_X\boldsymbol{\Phi}^{h+1'} \\ \boldsymbol{\Phi}^h\boldsymbol{\Sigma} & \boldsymbol{\Phi}^{h+1}\mathbf{V}_X\boldsymbol{\Gamma}' & \mathbf{V}_X \end{bmatrix} \right). \tag{C.1}$$

Using the properties of the multivariate normal distribution, we obtain:

$$\begin{aligned} & \mathbf{x}_{t+h}|\boldsymbol{\Gamma}\mathbf{x}_{t-1} = \mathbf{b}, \boldsymbol{\varepsilon}_t = \mathbf{d} \\ \sim\ & \mathcal{N}(\mathbb{E}(\mathbf{x}_{t+h}||\boldsymbol{\Gamma}\mathbf{x}_{t-1} = \mathbf{b}, \boldsymbol{\varepsilon}_t = \mathbf{d}), \mathbb{V}ar(\mathbf{x}_{t+h}||\boldsymbol{\Gamma}\mathbf{x}_{t-1} = \mathbf{b}, \boldsymbol{\varepsilon}_t = \mathbf{d})). \end{aligned} \tag{C.2}$$

[21] Specifically, we set $\alpha_\pi = 1.5$ and $\alpha_z = 0.5/12$. The latter reflects that our model is expressed in monthly returns, whereas z_t is independent of the model's frequency.

where $\mathbb{E}(\mathbf{x}_{t+h}||\mathbf{\Gamma}\mathbf{x}_{t-1}=\mathbf{b},\boldsymbol{\varepsilon}_t=\mathbf{d})$ is given by

$$\mathbf{e}_X+\left[\begin{array}{cc}\mathbf{\Phi}^h\mathbf{\Sigma} & \mathbf{\Phi}^{h+1}\mathbf{V}_X\mathbf{\Gamma}'\end{array}\right]\left[\begin{array}{cc}\boldsymbol{I} & \mathbf{0}\\ \mathbf{0} & \mathbf{\Gamma}\mathbf{V}_X\mathbf{\Gamma}'\end{array}\right]^{-1}\left(\left[\begin{array}{c}\mathbf{d}\\ \mathbf{b}\end{array}\right]-\left[\begin{array}{c}\mathbf{0}\\ \mathbf{\Gamma}\mathbf{e}_X\end{array}\right]\right),$$

and $\mathbb{V}ar(\mathbf{x}_{t+h}||\mathbf{\Gamma}\mathbf{x}_{t-1}=\mathbf{b},\boldsymbol{\varepsilon}_t=\mathbf{d})$ is equal to

$$\mathbf{V}_X-\left[\begin{array}{cc}\mathbf{\Phi}^h\mathbf{\Sigma} & \mathbf{\Phi}^{h+1}\mathbf{V}_X\mathbf{\Gamma}'\end{array}\right]\left[\begin{array}{cc}\boldsymbol{I} & \mathbf{0}\\ \mathbf{0} & \mathbf{\Gamma}\mathbf{V}_X\mathbf{\Gamma}'\end{array}\right]^{-1}\left[\begin{array}{cc}\mathbf{\Phi}^h\mathbf{\Sigma} & \mathbf{\Phi}^{h+1}\mathbf{V}_X\mathbf{\Gamma}'\end{array}\right]'.$$

A second-order Taylor expansion of $q(\mathbf{x}_{t+h})$ around $\mathbb{E}(\mathbf{x}_{t+h}|\mathcal{I}_t)$ is:

$$\begin{aligned}q(\mathbf{x}_{t+h}) &\approx q(\mathbb{E}(\mathbf{x}_{t+h}|\mathcal{I}_t))+(\mathbf{x}_{t+h}-\mathbb{E}(\mathbf{x}_{t+h}|\mathcal{I}_t))'\frac{\partial}{\partial\mathbf{x}_t}q(\mathbb{E}(\mathbf{x}_{t+h}|\mathcal{I}_t))+\\ &\quad\frac{1}{2}(\mathbf{x}_{t+h}-\mathbb{E}(\mathbf{x}_{t+h}|\mathcal{I}_t))'\frac{\partial^2}{\partial\mathbf{x}_t\partial\mathbf{x}_t'}q(\mathbb{E}(\mathbf{x}_{t+h}|\mathcal{I}_t))(\mathbf{x}_{t+h}-\mathbb{E}(\mathbf{x}_{t+h}|\mathcal{I}_t)).\end{aligned}$$

This implies that, for any conditioning information set $\mathcal{I}_t$:

$$\mathbb{E}(q(\mathbf{x}_{t+h})|\mathcal{I}_t) \approx q(\mathbb{E}(\mathbf{x}_{t+h}|\mathcal{I}_t))+\frac{1}{2}\operatorname{vec}\left[\frac{\partial^2}{\partial\mathbf{x}_t\partial\mathbf{x}_t'}q(\mathbb{E}(\mathbf{x}_{t+h}|\mathcal{I}_t))\right]'\operatorname{vec}\left[\mathbb{V}ar(\mathbf{x}_{t+h}|\mathcal{I}_t)\right].$$

In our specific case, $q(\mathbf{x}_t)$ corresponds to a nominal or real zero-coupon yield, of the form:

$$q(\mathbf{x}_t)=\frac{1}{h}(F_{0,1,t}+\cdots+F_{h-1,h,t}),$$

where $F_{n-1,n,t}$ is defined in Lemma 1. To compute the derivatives of q, we use that:

$$\frac{\partial}{\partial\mathbf{x}_t}F_{n-1,n,t} = \Phi^{\mathcal{N}}\left(\frac{a_n+\mathbf{b}_n'\mathbf{x}_t-\underline{i}}{\sigma_n}\right)\mathbf{b}_n-\mathbf{c}_n+\frac{\mathbf{b}'\mathbf{\Phi}_n\mathbf{\Sigma}\mathbf{\Sigma}'\mathbf{\Phi}_n'\mathbf{c}}{\sigma_n}\phi^{\mathcal{N}}\left(\frac{\bar{a}_n+\mathbf{b}_n'\mathbf{x}_t-\underline{i}}{\sigma_n}\right)\mathbf{b}_n.$$

$$\begin{aligned}&\frac{\partial^2}{\partial\mathbf{x}_t\partial\mathbf{x}_t'}F_{n-1,n,t}\\ =\ &\frac{1}{\sigma_n}\left(\phi^{\mathcal{N}}\left(\frac{a_n+\mathbf{b}_n'\mathbf{x}_t-\underline{i}}{\sigma_n}\right)-\frac{\mathbf{b}'\mathbf{\Phi}_n\mathbf{\Sigma}\mathbf{\Sigma}'\mathbf{\Phi}_n'\mathbf{c}}{\sigma_n}\left(\frac{\bar{a}_n+\mathbf{b}_n'\mathbf{x}_t-\underline{i}}{\sigma_n}\right)\phi^{\mathcal{N}}\left(\frac{\bar{a}_n+\mathbf{b}_n'\mathbf{x}_t-\underline{i}}{\sigma_n}\right)\right)(\mathbf{b}_n\mathbf{b}_n').\end{aligned}$$

References

Adrian, T., R. K. Crump, and E. Moench (2013). Pricing the Term Structure with Linear Regressions. *Journal of Financial Economics 110*(1), 110–138.

Ahn, D.-H., R. F. Dittmar, and A. R. Gallant (2002). Quadratic Term Structure Models: Theory and Evidence. *Review of Financial Studies 15*(1), 243–288.

Andreasen, M. M. and A. Meldrum (2019). A Shadow Rate or a Quadratic Policy Rule? The Best Way to Enforce the Zero Lower Bound in the United States. *Journal of Financial and Quantitative Analysis 54*(5), 2261–2292.

Ang, A., G. Bekaert, and M. Wei (2008). The Term Structure of Real Rates and Expected Inflation. *Journal of Finance 63*(2), 797–849.

Ang, A. and M. Piazzesi (2003). A No-Arbitrage Vector Autoregression of Term Structure Dynamics with Macroeconomic and Latent Variables. *Journal of Monetary Economics 50*(4), 745–787.

Bauer, M. D. and G. D. Rudebusch (2016). Monetary Policy Expectations at the Zero Lower Bound. *Journal of Money, Credit and Banking 48*(7), 1439–1465.

Bauer, M. D. and G. D. Rudebusch (2020). Interest Rates under Falling Stars. *American Economic Review 110*(5), 1316–1354.

Bauer, M. D., G. D. Rudebusch, and J. C. Wu (2012). Correcting Estimation Bias in Dynamic Term Structure Models. *Journal of Business & Economic Statistics 30*(3), 454–467.

Bianchi, F., L. Melosi, and M. Rottner (2021). Hitting the Elusive Inflation Target. *Journal of Monetary Economics 124*(C), 107–122.

Bielecki, M., M. Brzoza-Brzezina, and M. Kolasa (2023). Demographics, Monetary Policy, and the Zero Lower Bound. *Journal of Money, Credit and Banking 55*(7), 1857–1887.

Black, F. (1995). Interest Rates as Options. *Journal of Finance 50*(5), 1371–76.

Bletzinger, T., W. Lemke, and J.-P. Renne (2025). Time-Varying Risk Aversion and Inflation-Consumption Correlation in an Equilibrium Term Structure Model. *Journal of Financial Econometrics forthcoming*.

Brave, S. A., R. A. Butters, and D. Kelley (2019). A New "Big Data"' Index of U.S. Economic Activity. *Economic Perspectives* (1), 1–30.

Brayton, F., T. Laubach, and D. Reifschneider (2014). The FRB/US Model: A Tool for Macroeconomic Policy Analysis. FEDS Notes, Board of Governors of the Federal Reserve System.

Breach, T., S. D'Amico, and A. Orphanides (2020). The Term Structure and Inflation Uncertainty. *Journal of Financial Economics 138*(2), 388–414.

Campbell, J. Y., A. W. Lo, and A. MacKinlay (1997). *The Econometrics of Financial Markets*. Princeton University Press.

Campbell, J. Y. and L. M. Viceira (2001). Who Should Buy Long-Term Bonds? *American Economic Review 91*(1), 99–127.

Carriero, A., S. Mouabbi, and E. Vangelista (2018). UK Term Structure Decompositions at the Zero Lower Bound. *Journal of Applied Econometrics 33*(5), 643–661.

Chernov, M. and P. Mueller (2012). The Term Structure of Inflation Expectations. *Journal of Financial Economics 106*(2), 367–394.

Christensen, J. H. E., J. A. Lopez, and G. D. Rudebusch (2010). Inflation Expectations and Risk Premiums in an Arbitrage-Free Model of Nominal and Real Bond Yields. *Journal of Money, Credit and Banking 42*(s1), 143–178.

Christensen, J. H. E., J. A. Lopez, and G. D. Rudebusch (2016). Pricing Deflation Risk with US Treasury Yields. *Review of Finance 20*(3), 1107–1152.

Christensen, J. H. E. and G. D. Rudebusch (2015). Estimating Shadow-Rate Term Structure Models with Near-Zero Yields. *The Journal of Financial Econometrics 13*(2), 226–259.

Christensen, J. H. E. and G. D. Rudebusch (2016). Modeling Yields at the Zero Lower Bound: Are Shadow Rates the Solution? In *Dynamic Factor Models*, Volume 35 of *Advances in Econometrics*, pp. 75–125. Emerald Group Publishing Limited.

Chung, H., J. Laforte, D. Reifschneider, and J. C. Williams (2012). Have We Underestimated the Likelihood and Severity of Zero Lower Bound Events? *Journal of Money, Credit and Banking 44*(s1), 47–82.

Cox, J. C., J. E. Ingersoll, and S. A. Ross (1985). An Intertemporal General Equilibrium Model of Asset Prices. *Econometrica 53*(2), 363–84.

Dai, Q., A. Le, and K. J. Singleton (2010). Discrete-Time Affine-Q Term Structure Models with Generalized Market Prices of Risk. *Review of Financial Studies 23*(5), 2184–2227.

Dai, Q. and K. J. Singleton (2000). Specification Analysis of Affine Term Structure Models. *Journal of Finance 55*(5), 1943–1978.

D'Amico, S., D. H. Kim, and M. Wei (2018). Tips from TIPS: The Informational Content of Treasury Inflation-Protected Security Prices. *Journal of Financial and Quantitative Analysis 53*(1), 395–436.

Dewachter, H. and M. Lyrio (2006). Macro Factors and the Term Structure of Interest Rates. *Journal of Money, Credit and Banking 38*(1), 119–140.

Diebold, F., G. Rudebusch, and S. B. Aruoba (2006). The Macroeconomy and the Yield Curve: a Dynamic Latent Factor Approach. *Journal of Econometrics 131*(1-2), 309–338.

Evans, M. D. D. (2003). Real Risk, Inflation Risk, and the Term Structure. *The Economic Journal 113*(487), 345–389.

Fama, E. F. and M. R. Gibbons (1982). Inflation, Real Returns and Capital Investment. *Journal of Monetary Economics 9*(3), 297–323.

Fernández-Villaverde, J., J. Marbet, G. Nuño, and O. Rachedi (2023). Inequality and the Zero Lower Bound. NBER Working Papers 31282, National Bureau of Economic Research, Inc.

Fries, S., J. Mésonnier, S. Mouabbi, and J. Renne (2018). National Natural Rates of Interest and the Single Monetary Policy in the Euro Area. *Journal of Applied Econometrics 33*(6), 763–779.

Goliński, A. and P. Spencer (2024). Unconventional Monetary Policies and the Yield Curve: Estimating Non-Affine Term Structure Models with Unspanned Macro Risk by Factor Extraction. *The Review of Asset Pricing Studies 14*(1), 119–152.

Gorodnichenko, Y. and B. Lee (2017, November). A Note on Variance Decomposition with Local Projections. NBER Working Papers 23998, National Bureau of Economic Research, Inc.

Gouriéroux, C. and J. Jasiak (2006). Autoregressive Gamma Processes. *Journal of Forecasting 25*, 129–152.

Grishchenko, O. V., J. M. Vanden, and J. Zhang (2016). The iInformational Content of the Embedded Deflation Option in TIPS. *Journal of Banking & Finance 65*(C), 1–26.

Groen, J. J. J. and M. Middeldorp (2013). Creating a History of U.S. Inflation Expectations. Liberty Street Economics 20130821, Federal Reserve Bank of New York.

Gürkaynak, R. S., B. Sack, and J. H. Wright (2007). The U.S. Treasury Yield Curve: 1961 to the Present. *Journal of Monetary Economics 54*(8), 2291–2304.

Gürkaynak, R. S., B. Sack, and J. H. Wright (2010). The TIPS Yield Curve and Inflation Compensation. *American Economic Journal: Macroeconomics 2*(1), 70–92.

Gürkaynak, R. S. and J. H. Wright (2012). Macroeconomics and the Term Structure. *Journal of Economic Literature 50*(2), 331–367.

Herwartz, H., S. Maxand, and H. Rohloff (2022). The Link between Monetary Policy, Stock Prices, and House Prices–Evidence from a Statistical Identification Approach. *International Journal of Central Banking 18*(5), 1–53.

Holston, K., T. Laubach, and J. C. Williams (2017). Measuring the Natural Rate of Interest: International Trends and Determinants. *Journal of International Economics 108*, S59–S75.

Hördahl, P. and O. Tristani (2012). Inflation Risk Premia in the Term Structure of Interest Rates. *Journal of the European Economic Association 10*(3), 634–657.

Hördahl, P., O. Tristani, and D. Vestin (2006). A Joint Econometric Model of Macroeconomic and Term-Structure Dynamics. *Journal of Econometrics 131*(1), 405–444.

Ichiue, H. and Y. Ueno (2007). Equilibrium Yield Curve and the Yield Curve in Low Interest Rate Environment. Working paper series, Bank of Japan.

Ichiue, H. and Y. Ueno (2013). Estimating Term Premia at the Zero Bound: An Analysis of Japanese, U.S. and U.K. Yields. Working paper series, Bank of Japan.

Imakubo, K. and J. Nakajima (2015). Estimating Inflation Risk Premia from Nominal and Real Yield Curves Using a Shadow-Rate Model. Bank of Japan Working Paper Series 15-E-1, Bank of Japan.

Jardet, C., A. Monfort, and F. Pegoraro (2013). No-Arbitrage Near-Cointegrated VAR(p) Term Structure Models, Term Premia and GDP Growth. *Journal of Banking & Finance 37*(2), 389–402.

Joslin, S., M. Priebsch, and K. J. Singleton (2014). Risk Premiums in Dynamic Term Structure Models with Unspanned Macro Risks. *Journal of Finance 69*, 1197–1233.

Kim, D. H. and A. Orphanides (2012). Term Structure Estimation with Survey Data on Interest Rate Forecasts. *Journal of Financial and Quantitative Analysis 47*(01), 241–272.

Kim, D. H. and M. A. Priebsch (2013). Estimation of Multi-Factor Shadow-Rate Term Structure Models. Technical report, Board of Governors of the Federal Reserve System (U.S.).

Kim, D. H. and K. J. Singleton (2012). Term Structure Models and the Zero Bound: An Empirical Investigation of Japanese Yields. *Journal of Econometrics 170*(1), 32–49.

Kim, D. H. and J. H. Wright (2005). An Arbitrage-Free Three-Factor Term Structure Model and the Recent Behavior of Long-Term Yields and Distant-Horizon Forward Rates. Finance and Economics Discussion Series 2005-33, Board of Governors of the Federal Reserve System (U.S.).

Krippner, L. (2012, March). Modifying Gaussian Term Structure Models When Interest Rates are Near the Zero Lower Bound. Reserve Bank of New Zealand Discussion Paper Series DP2012/02, Reserve Bank of New Zealand.

Krippner, L. (2013). Measuring the Stance of Monetary Policy in Zero Lower Bound Environments. *Economics Letters 118*(1), 135–138.

Laubach, T. and J. C. Williams (2003). Measuring the Natural Rate of Interest. *The Review of Economics and Statistics 85*(4), 1063–1070.

Leippold, M. and L. Wu (2002). Asset Pricing under the Quadratic Class. *Journal of Financial and Quantitative Analysis 37*(02), 271–295.

Lemke, W. and A. L. Vladu (2017, January). Below the Zero Lower Bound: a Shadow-Rate Term Structure Model for the Euro Area. Working Paper Series 1991, European Central Bank.

Mésonnier, J.-S. and J.-P. Renne (2007). A Time-Varying Natural Rate of Interest for the Euro Area. *European Economic Review 51*(7), 1768–1784.

Monfort, A., F. Pegoraro, J.-P. Renne, and G. Roussellet (2017). Staying at Zero with Affine Processes: An Application to Term-Structure Modelling. *Journal of Econometrics 201*(2), 348–366.

Mundell, R. (1963). Inflation and Real Interest. *Journal of Political Economy 71*(3), 280–283.

Orphanides, A. (2007). Taylor Rules. Finance and Economics Discussion Series 2007-18, Board of Governors of the Federal Reserve System (U.S.).

Pallara, K. and J.-P. Renne (2024). Fiscal Limits and the Pricing of Eurobonds. *Management Science 70*(2), 1216–1237.

Pearson, N. D. and T.-S. Sun (1994). Exploiting the Conditional Density in Estimating the Term Structure: An Application to the Cox, Ingersoll, and Ross Model. *Journal of Finance 49*(4), 1279–1304.

Potter, S. M. (2000). Nonlinear Impulse Response Functions. *Journal of Economic Dynamics and Control 24*(10), 1425–1446.

Priebsch, M. A. (2013). Computing Arbitrage-Free Yields in Multi-Factor Gaussian Shadow-Rate Term Structure Models. Finance and Economics Discussion Series 2013-63, Board of Governors of the Federal Reserve System (U.S.).

Rachel, L. and L. H. Summers (2019). On Secular Stagnation in the Industrialized World. NBER Working Papers 26198, National Bureau of Economic Research, Inc.

Renne, J.-P. and K. Pallara (2023). Fiscal Fatigue, Fiscal Limits and Sovereign Credit Spreads. Technical report, University of Lausanne.

Rogoff, K. S., B. Rossi, and P. Schmelzing (2024). Rethinking Short-Term Real Interest Rates and Term Spreads Using Very Long-Run Data. NBER Working Papers 33079, National Bureau of Economic Research, Inc.

Roussellet, G. (2023). The Term Structure of Macroeconomic Risks at the Effective Lower Bound. *Journal of Econometrics*, 105383.

Rudebusch, G. D. and T. Wu (2008). A Macro-Finance Model of the Term Structure, Monetary Policy and the Economy. *Economic Journal 118*(530), 906–926.

Shapiro, A. H. and D. J. Wilson (2022). Taking the Fed at its Word: A New Approach to Estimating Central Bank Objectives using Text Analysis. *The Review of Economic Studies 89*(5), 2768–2805.

Sims, E. and J. Wu (2020). Federal Reserve Policy in a World of Low Interest Rates. *Cato Journal 40*(2), 343–360.

Tobin, J. (1965). Money and Economic Growth. *Econometrica 33*(4), 671–684.

Uhlig, H. (2005). What Are the Effects of Monetary Policy on Output? Results From an Agnostic Identification Procedure. *Journal of Monetary Economics 52*, 381–419.

Uhlig, H. and P. Amir-Ahmadi (2012). Measuring The Dynamic Effects Of Monetary Policy Shocks: A Bayesian Favar Approach With Sign Restriction. 2012 Meeting Papers 1060, Society for Economic Dynamics.

Wu, J. C. and F. D. Xia (2016). Measuring the Macroeconomic Impact of Monetary Policy at the Zero Lower Bound. *Journal of Money, Credit and Banking 48*(2-3), 253–291.

Wu, J. C. and F. D. Xia (2020). Negative Interest Rate Policy and the Yield Curve. *Journal of Applied Econometrics 35*(6), 653–672.

Wu, J. C. and J. Zhang (2019). A Shadow Rate New Keynesian Model. *Journal of Economic Dynamics and Control 107*(C).

— Supplementary Material —

The Shadow-Rate Model: Let's Make it Real

Adam GOLINSKI, Sophie GUILLOUX-NEFUSSI, and Jean-Paul RENNE

I. Proof of Lemma 1 (Extension of Wu and Xia (2016))

Proof. We have

$$K_h(\mathbf{x}_t, a, \mathbf{b}, \mathbf{c}) = \exp(-f_{0,1,t} - \cdots - f_{h-1,h,t}),$$

where, for $n \in \{1, \ldots, h\}$,

$$f_{n-1,n,t} = -\log K_n(\mathbf{x}_t, a, \mathbf{b}, \mathbf{c}) + \log K_{n-1}(\mathbf{x}_t, a, \mathbf{b}, \mathbf{c}).$$

We look for an approximation to the $f_{n-1,n,t}$'s. For that, we use the fact that, for any random variable z, we have $\log \mathbb{E}(\exp(z)) \approx \mathbb{E}(z) + \frac{1}{2}\mathbb{V}ar(z)$—the approximation being exact when z is Gaussian (which is not the case here due to the max operator). This gives the following approximation to $f_{n-1,n,t}$:

$$\begin{aligned}
&\mathbb{E}\left[\max(\underline{\ell}, b + \mathbf{b}'\mathbf{w}_{t+n}) - \mathbf{c}'\mathbf{w}_{t+n} \,\middle|\, \underline{\mathbf{w}_t}\right] \\
&-\frac{1}{2}\mathbb{V}ar_t\Big[-\max(\underline{\ell}, a + \mathbf{b}'\mathbf{w}_{t+1}) - \cdots - \max(\underline{\ell}, a + \mathbf{b}'\mathbf{w}_{t+n}) + \mathbf{c}'\mathbf{w}_{t+1} + \cdots + \mathbf{c}'\mathbf{w}_{t+n}\Big] \\
&+\frac{1}{2}\mathbb{V}ar_t\Big[-\max(\underline{\ell}, a + \mathbf{b}'\mathbf{w}_{t+1}) - \cdots - \max(\underline{\ell}, a + \mathbf{b}'\mathbf{w}_{t+n-1}) + \mathbf{c}'\mathbf{w}_{t+1} + \cdots + \mathbf{c}'\mathbf{w}_{t+n-1}\Big].
\end{aligned}$$

Without the max operator, the sum of the two variance terms would be equal to:

$$\begin{aligned}
&-\frac{1}{2}\left\{\mathbb{V}ar\left([\mathbf{c}-\mathbf{b}]'\mathbf{w}_{t+n} \,\middle|\, \underline{\mathbf{w}_t}\right) + 2\sum_{k=1}^{n-1}\mathbb{C}ov\left([\mathbf{c}-\mathbf{b}]'\mathbf{w}_{t+k}, [\mathbf{c}-\mathbf{b}]'\mathbf{w}_{t+n} \,\middle|\, \underline{\mathbf{w}_t}\right)\right\} \\
= \quad &-\frac{1}{2}(\mathbf{c}-\mathbf{b})'\left(\sum_{k=0}^{n-1}\mathbf{\Phi}^k\right)\mathbf{\Sigma}\left(\sum_{k=0}^{n-1}\mathbf{\Phi}^k\right)'(\mathbf{c}-\mathbf{b}) = -\frac{1}{2}(\mathbf{c}-\mathbf{b})'\mathbf{\Phi}_n\mathbf{\Sigma}\mathbf{\Phi}_n'(\mathbf{c}-\mathbf{b}).
\end{aligned}$$

Conversely, if the max terms were all equal to $\underline{\ell}$, the variance terms would be equal to $-\mathbf{c}'\mathbf{\Phi}_n\mathbf{\Sigma}\mathbf{\Phi}_n'\mathbf{c}/2$.

Following Wu and Xia (2016), and assuming that $\mathbf{b}'\mathbf{w}_t$ is a persistent process, we obtain the following approximation to the sum of the two variance terms:

$$-\frac{1}{2}\left\{p_{t,n}(\mathbf{c}-\mathbf{b})'\mathbf{\Phi}_n\mathbf{\Sigma}\mathbf{\Sigma}'\mathbf{\Phi}_n'(\mathbf{c}-\mathbf{b}) + (1-p_{t,n})\mathbf{c}'\mathbf{\Phi}_n\mathbf{\Sigma}\mathbf{\Sigma}'\mathbf{\Phi}_n'\mathbf{c}\right\},$$

where $p_{t,n} = \mathbb{P}_t(a + \mathbf{b}'\mathbf{w}_{t+n} > \underline{\ell})$.

At that stage, we have:

$$\begin{aligned} f_{n-1,n,t} &\approx \mathbb{E}_t\left[\max(\underline{\ell}, a + \mathbf{b}'\mathbf{w}_{t+n})\right] - \mathbf{c}'\mathbb{E}_t(\mathbf{w}_{t+n}) - \frac{1}{2}\mathbf{c}'\mathbf{\Phi}_n\mathbf{\Sigma}\mathbf{\Phi}_n'\mathbf{c} \\ &\quad + p_{t,n}\mathbf{b}'\mathbf{\Phi}_n\mathbf{\Sigma}\mathbf{\Phi}_n'\mathbf{c} - \frac{p_{t,n}}{2}\mathbf{b}'\mathbf{\Phi}_n\mathbf{\Sigma}\mathbf{\Phi}_n'\mathbf{b}. \end{aligned} \tag{I.1}$$

It is easily checked that $a + \mathbf{b}'\mathbb{E}_t(\mathbf{w}_{t+n}) = \bar{a}_n + \mathbf{b}_n'\mathbf{w}_t$, where $\bar{a}_n$ and $\mathbf{b}_n$ given in (A.1). Therefore:

$$a + \mathbf{b}'\mathbf{w}_{t+n}|\mathcal{I}_t \sim \mathcal{N}\left[a + \mathbf{b}'\mathbb{E}_t(\mathbf{w}_{t+n}), \sigma_n^2\right], \quad \text{with} \quad \sigma_n^2 = \mathbb{V}ar_t(a + \mathbf{b}'\mathbf{w}_{t+n}).$$

Using standard results regarding the truncated normal distribution, we then obtain:

$$\mathbb{E}_t(\max(\underline{\ell}, a + \mathbf{b}'\mathbf{w}_{t+n})) - \underline{\ell} = \sigma_n g\left(\frac{\bar{a}_n + \mathbf{b}_n'\mathbf{w}_t - \underline{\ell}}{\sigma_n}\right).$$

Since $g' = \Phi^{\mathcal{N}}$, where $\Phi^{\mathcal{N}}$ is the cumulative distribution function of $\mathcal{N}(0,1)$, we have $p_{t,n} = \Phi^{\mathcal{N}}[(\bar{a}_n + \mathbf{b}_n'\mathbf{w}_t - \underline{\ell})/\sigma_n] = g'[(\bar{a}_n + \mathbf{b}_n'\mathbf{w}_t - \underline{\ell})/\sigma_n]$. Therefore, the last term of (I.1) rewrites:

$$-\frac{p_{t,n}}{2}\mathbf{b}'\mathbf{\Phi}_n\mathbf{\Sigma}\mathbf{\Phi}_n'\mathbf{b} = g'\left(\frac{\bar{a}_n + \mathbf{b}_n'\mathbf{w}_t - \underline{\ell}}{\sigma_n}\right)(a_n - \bar{a}_n),$$

where we have used that $a_n - \bar{a}_n = -\mathbf{b}'\mathbf{\Phi}_n\mathbf{\Sigma}\mathbf{\Phi}_n'\mathbf{b}/2$.

Therefore,

$$\begin{aligned} &\mathbb{E}_t\left[\max(\underline{\ell}, a + \mathbf{b}'\mathbf{w}_{t+n})\right] - \underline{\ell} - \frac{p_{t,n}}{2}\mathbf{b}'\mathbf{\Phi}_n\mathbf{\Sigma}\mathbf{\Phi}_n'\mathbf{b} \\ = \;& \sigma_n\left(g\left(\frac{\bar{a}_n + \mathbf{b}_n'\mathbf{w}_t - \underline{\ell}}{\sigma_n}\right) + \frac{a_n - \bar{a}_n}{\sigma_n}g'\left(\frac{\bar{a}_n + \mathbf{b}_n'\mathbf{w}_t - \underline{\ell}}{\sigma_n}\right)\right) \approx \sigma_n g\left(\frac{a_n + \mathbf{b}_n'\mathbf{w}_t - \underline{\ell}}{\sigma_n}\right). \end{aligned}$$

Equation (I.1) then rewrites:

$$f_{n-1,n,t} \approx \underline{\ell} + \sigma_n g\left(\frac{a_n + \mathbf{b}_n'\mathbf{w}_t - \underline{\ell}}{\sigma_n}\right) - (\dot{c}_n + \mathbf{c}_n'\mathbf{w}_t) + p_{t,n}\mathbf{b}'\mathbf{\Phi}_n\mathbf{\Sigma}\mathbf{\Phi}_n'\mathbf{c},$$

with

$$\dot{c}_n + \mathbf{c}_n'\mathbf{w}_t = \mathbf{c}'\mathbb{E}_t(\mathbf{w}_{t+n}) + \frac{1}{2}\mathbf{c}'\mathbf{\Phi}_n\mathbf{\Sigma}\mathbf{\Phi}_n'\mathbf{c},$$

which leads to the result. □

II. Matrix representation of the model

First note that we have:

$$\begin{aligned}
& \mathbb{E}(\pi_t|\mathcal{I}_{t-1}) \\
= \; & \mathbb{E}(\bar{\pi}_t + u_t|\mathcal{I}_{t-1}) = \mathbb{E}((1-\bar{\rho})\pi_t^* + \bar{\rho}\bar{\pi}_{t-1} + \beta z_{t-1} + a_1\varepsilon_{u,t-1} + \cdots + a_p\varepsilon_{u,t-p}|\mathcal{I}_{t-1}) \\
= \; & (1-\bar{\rho})[(1-\rho^*)\mu^* + \rho^*\pi_{t-1}^*] + \bar{\rho}\bar{\pi}_{t-1} + \beta z_{t-1} + \mathbf{a}'\boldsymbol{\varepsilon}_{u,t} \\
= \; & (1-\bar{\rho})(1-\rho^*)\mu^* + (1-\bar{\rho})\rho^*\pi_{t-1}^* + \bar{\rho}\bar{\pi}_{t-1} + \beta z_{t-1} + \mathbf{a}'\mathbf{J}_0\boldsymbol{\varepsilon}_{u,t-1},
\end{aligned}$$

where

$$\mathbf{J}_0 = \begin{bmatrix} \mathbf{0}_{1\times p} & 0 \\ \boldsymbol{I}_p & \mathbf{0}_{p\times 1} \end{bmatrix}.$$

Therefore, (15) rewrites:

$$\begin{aligned}
z_t &= \rho_z z_{t-1} - \alpha s_{t-1} + \alpha\mathbb{E}(\pi_t|\mathcal{I}_{t-1}) + \alpha r_{t-1}^* + \sigma_z\varepsilon_{z,t} \\
&= \alpha(1-\bar{\rho})(1-\rho^*)\mu^* + (\rho_z + \alpha\beta)z_{t-1} + \alpha(1-\bar{\rho})\rho^*\pi_{t-1}^* + \alpha\bar{\rho}\bar{\pi}_{t-1} + \alpha\mathbf{a}'\mathbf{J}_0\boldsymbol{\varepsilon}_{u,t-1} \\
&\quad -\alpha s_{t-1} + \alpha r_{t-1}^* + \sigma_z\varepsilon_{z,t}.
\end{aligned}$$

Eq. (1), combined with the e macroeconomic equations presented in Subsection 3, and with the nominal SDF (4)—with the price of risk specification of (23)—completely define the model.

The state vector is

$$\mathbf{x}_t = [s_t, s_{t-1}, \kappa_t, g_t, z_t, z_{t-1}, \pi_t^*, r_t^*, \bar{\pi}_t, \varepsilon_{u,t}, \ldots, \varepsilon_{u,t-p}, w_t]'.$$

The model admits the following representation:

$$\mathbf{A}\mathbf{x}_t = \tilde{\boldsymbol{\mu}} + \tilde{\boldsymbol{\Phi}}\mathbf{x}_{t-1} + \tilde{\boldsymbol{\Sigma}}\boldsymbol{\varepsilon}_t.$$

where

$$\mathbf{A} = \begin{bmatrix}
1 & 0 & 0 & 0 & -\rho_i\alpha_z & 0 & -\rho_i(1-\alpha_\pi) & -\rho_i & -\rho_i\alpha_\pi & -\rho_i\alpha_\pi\mathbf{a}' & 0 \\
0 & 1 & 0 & 0 & 0 & 0 & 0 & 0 & 0 & \mathbf{0} & 0 \\
0 & 0 & 1 & 0 & 0 & 0 & 0 & 0 & 0 & \mathbf{0} & 0 \\
0 & 0 & 0 & 1 & 0 & 0 & 0 & 0 & 0 & \mathbf{0} & 0 \\
0 & 0 & 0 & 0 & 1 & 0 & 0 & 0 & 0 & \mathbf{0} & 0 \\
0 & 0 & 0 & 0 & 0 & 1 & 0 & 0 & 0 & \mathbf{0} & 0 \\
0 & 0 & 0 & 0 & 0 & 0 & 1 & 0 & 0 & \mathbf{0} & 0 \\
0 & 0 & -1 & 0 & 0 & 0 & 0 & 1 & 0 & \mathbf{0} & 0 \\
0 & 0 & 0 & 0 & 0 & 0 & -(1-\bar{\rho}) & 0 & 1 & \mathbf{0} & 0 \\
\mathbf{0} & \mathbf{0} & \mathbf{0} & \mathbf{0} & \mathbf{0} & \mathbf{0} & \mathbf{0} & \mathbf{0} & \mathbf{0} & \boldsymbol{I}_{p+1} & \mathbf{0} \\
0 & 0 & 0 & 0 & 0 & 0 & 0 & 0 & 0 & \mathbf{0} & 1
\end{bmatrix},$$

$$\tilde{\boldsymbol{\mu}} = \begin{bmatrix} 0 \\ 0 \\ (1-\rho_\kappa)\mu_\kappa \\ (1-\rho_g)\mu_g \\ \alpha(1-\bar{\rho})(1-\rho^*)\mu^* \\ 0 \\ (1-\rho^*)\mu^* \\ \mu_\kappa + \theta(1-\rho_g)\mu_g \\ 0 \\ \mathbf{0}_{(p+1)\times 1} \\ (1-\rho_w)\mu_w \end{bmatrix}, \quad \tilde{\boldsymbol{\Phi}} = \begin{bmatrix} (1-\rho_i) & 0 & 0 & 0 & 0 & 0 & 0 & 0 & 0 & \mathbf{0} & 0 \\ 1 & 0 & 0 & 0 & 0 & 0 & 0 & 0 & 0 & \mathbf{0} & 0 \\ 0 & 0 & \rho_\kappa & 0 & 0 & 0 & 0 & 0 & 0 & \mathbf{0} & 0 \\ 0 & 0 & 0 & \rho_g & 0 & 0 & 0 & 0 & 0 & \mathbf{0} & 0 \\ -\alpha & 0 & 0 & 0 & \alpha\beta + \rho_z & 0 & \alpha(1-\bar{\rho})\rho^* & \alpha & \alpha\bar{\rho} & \alpha\mathbf{a}'\mathbf{J}_0 & 0 \\ 0 & 0 & 0 & 0 & 1 & 0 & 0 & 0 & 0 & \mathbf{0} & 0 \\ 0 & 0 & 0 & 0 & 0 & 0 & \rho^* & 0 & 0 & \mathbf{0} & 0 \\ 0 & 0 & 0 & \theta\rho_g & 0 & 0 & 0 & 0 & 0 & \mathbf{0} & 0 \\ 0 & 0 & 0 & 0 & \beta & 0 & 0 & 0 & \bar{\rho} & \mathbf{0} & 0 \\ \mathbf{0} & \mathbf{0} & \mathbf{0} & \mathbf{0} & \mathbf{0} & \mathbf{0} & \mathbf{0} & \mathbf{0} & \mathbf{0} & \mathbf{J}_0 & \mathbf{0} \\ 0 & 0 & 0 & 0 & 0 & 0 & 0 & 0 & 0 & \mathbf{0} & \rho_w \end{bmatrix}$$

$$\tilde{\boldsymbol{\Sigma}} = \begin{bmatrix} \sigma_i & 0 & 0 & 0 & 0 & 0 & 0 & 0 \\ 0 & 0 & 0 & 0 & 0 & 0 & 0 & 0 \\ 0 & 0 & 0 & 0 & 0 & 0 & 0 & \sigma_\kappa \\ 0 & \sigma_g & 0 & 0 & 0 & 0 & 0 & 0 \\ 0 & 0 & \sigma_z & 0 & 0 & 0 & 0 & 0 \\ 0 & 0 & 0 & 0 & 0 & 0 & 0 & 0 \\ 0 & 0 & 0 & \sigma^* & 0 & 0 & 0 & 0 \\ 0 & \theta\sigma_g & 0 & 0 & 0 & 0 & 0 & 0 \\ 0 & 0 & 0 & 0 & \sigma_\pi & 0 & 0 & 0 \\ \mathbf{0} & \mathbf{0} & \mathbf{0} & \mathbf{0} & \mathbf{0} & \mathbf{J}_1 & \mathbf{0} & \mathbf{0} \\ 0 & \sigma_{w,g} & \sigma_{w,z} & 0 & \sigma_{w,\pi} & 0 & \sigma_w & 0 \end{bmatrix}, \quad \text{and} \quad \boldsymbol{\varepsilon}_t = \begin{bmatrix} \varepsilon_{i,t} \\ \varepsilon_{g,t} \\ \varepsilon_{z,t} \\ \varepsilon_t^* \\ \varepsilon_{\pi,t} \\ \varepsilon_{u,t} \\ \varepsilon_{w,t} \\ \varepsilon_{\kappa,t} \end{bmatrix},$$

where

$$\mathbf{J}_0 = \begin{bmatrix} \mathbf{0}_{1\times p} & 0 \\ \boldsymbol{I}_p & \mathbf{0}_{p\times 1} \end{bmatrix}, \quad \text{and} \quad \mathbf{J}_1 = \underbrace{\begin{bmatrix} 1 \\ 0 \\ \vdots \\ 0 \end{bmatrix}}_{(p+1)\times 1}.$$

This dynamics therefore satisfies (3) with:

$$\boldsymbol{\mu} = \mathbf{A}^{-1}\tilde{\boldsymbol{\mu}}, \quad \boldsymbol{\Phi} = \mathbf{A}^{-1}\tilde{\boldsymbol{\Phi}}, \quad \text{and} \quad \boldsymbol{\Sigma} = \mathbf{A}^{-1}\tilde{\boldsymbol{\Sigma}}.$$

III. Model-implied forecasts

This appendix gives formulas that can be used to derive model-implied forecasts. These formulas are used if the measurement equations of the state-space model include surveys.

Using (3), it comes that:

$$\boldsymbol{\mu}_{t,h} := \mathbb{E}_t(\mathbf{x}_{t+h}) = (\boldsymbol{I} - \boldsymbol{\Phi})^{-1}(\boldsymbol{I} - \boldsymbol{\Phi}^h)\boldsymbol{\mu} + \boldsymbol{\Phi}^h\mathbf{x}_t, \tag{III.1}$$

and that

$$\begin{aligned}\mathbb{E}_t(\mathbf{x}_{t+1}+\cdots+\mathbf{x}_{t+h}) &= (\boldsymbol{I}-\boldsymbol{\Phi})^{-1}\left[h\boldsymbol{I}-\boldsymbol{\Phi}(\boldsymbol{I}-\boldsymbol{\Phi})^{-1}(\boldsymbol{I}-\boldsymbol{\Phi}^h)\right]\boldsymbol{\mu}+\\ &\quad \boldsymbol{\Phi}(\boldsymbol{I}-\boldsymbol{\Phi})^{-1}(\boldsymbol{I}-\boldsymbol{\Phi}^h)\mathbf{x}_t. \qquad \text{(III.2)}\end{aligned}$$

Moreover, the conditional covariance matrices of $\mathbf{x}_t$ can be obtained by applying recursively:

$$\boldsymbol{\Gamma}_h := \mathbb{V}ar_t(\mathbf{x}_{t+h}) = \boldsymbol{\Sigma}\boldsymbol{\Sigma}' + \boldsymbol{\Phi}\boldsymbol{\Gamma}_{h-1}\boldsymbol{\Phi}', \quad \text{and} \quad \boldsymbol{\Gamma}_0 = \mathbf{0}. \qquad \text{(III.3)}$$

Let us now consider model-implied forecasts of the short-term nominal yield. According to (1) and (2), we have:

$$i_t = \max(\underline{i}, \delta_0 + \boldsymbol{\delta}_1'\mathbf{x}_t).$$

Conditionally on the information available at date t (denoted by $\mathcal{I}_t$), $\mathbf{x}_{t+h}$ is Gaussian, with a mean $\boldsymbol{\mu}_{t,h}$ that is given by (III.1), and a variance $\boldsymbol{\Gamma}_h$ given by (III.3). That is:

$$\mathbf{x}_{t+h}|\mathcal{I}_t \sim \mathcal{N}(\boldsymbol{\mu}_{t,h}, \boldsymbol{\Gamma}_h),$$

and:

$$\delta_0 + \boldsymbol{\delta}_1'\mathbf{x}_{t+h}|\mathcal{I}_t \sim \mathcal{N}(\delta_0 + \boldsymbol{\delta}_1'\boldsymbol{\mu}_{t,h}, \boldsymbol{\delta}_1'\boldsymbol{\Gamma}_h\boldsymbol{\delta}_1),$$

Using standard results on the truncated Laplace transform, it then comes that:

$$\begin{aligned}\mathbb{E}_t(i_{t+h}) &= \underline{i} + \Phi^{\mathcal{N}}\left(\frac{\delta_0+\boldsymbol{\delta}_1'\boldsymbol{\mu}_{t,h}-\underline{i}}{\sqrt{\boldsymbol{\delta}_1'\boldsymbol{\Gamma}_h\boldsymbol{\delta}_1}}\right)(\delta_0+\boldsymbol{\delta}_1'\boldsymbol{\mu}_{t,h}-\underline{i}) + \phi^{\mathcal{N}}\left(\frac{\delta_0+\boldsymbol{\delta}_1'\boldsymbol{\mu}_{t,h}-\underline{i}}{\sqrt{\boldsymbol{\delta}_1'\boldsymbol{\Gamma}_h\boldsymbol{\delta}_1}}\right)\sqrt{\boldsymbol{\delta}_1'\boldsymbol{\Gamma}_h\boldsymbol{\delta}_1}.\\ &= \underline{i} + \sqrt{\boldsymbol{\delta}_1'\boldsymbol{\Gamma}_h\boldsymbol{\delta}_1}\,g\left(\frac{\delta_0+\boldsymbol{\delta}_1'\boldsymbol{\mu}_{t,h}-\underline{i}}{\sqrt{\boldsymbol{\delta}_1'\boldsymbol{\Gamma}_h\boldsymbol{\delta}_1}}\right). \qquad \text{(III.4)}\end{aligned}$$

In the context of the extended Kalman filter, we need to differentiate the model-implied forecasts w.r.t. the state vector $\mathbf{x}_t$. Exploiting the fact that $g' = \Phi^{\mathcal{N}}$ (the c.d.f. of $\mathcal{N}(0,1)$), we have:

$$\frac{\partial}{\partial \mathbf{x}_t}\mathbb{E}_t(i_{t+h}) = \Phi^{\mathcal{N}}\left(\frac{\delta_0+\boldsymbol{\delta}_1'\boldsymbol{\mu}_{t,n}-\underline{i}}{\sqrt{\boldsymbol{\delta}_1'\boldsymbol{\Gamma}_{n,0}\boldsymbol{\delta}_1}}\right)\boldsymbol{\delta}_1.$$

IV. Using the pricing formulas of Lemma 1 in the context of the model of Section 3

The shadow rate is $s_t = \delta_0 + \boldsymbol{\delta}_1'\mathbf{x}_t$ (this is eq. 2), with:

$$\delta_0 = 0, \quad \text{and} \quad \boldsymbol{\delta}_1 = [1, 0, \dots]'.$$

We also have $s_{t-1} = \delta_0 + \tilde{\delta}_1{}' \mathbf{x}_t$, with:

$$\delta_0 = 0, \quad \text{and} \quad \tilde{\delta}_1 = [0, 1, 0, \dots]'.$$

Inflation (eq. 20) is given by $\pi_t = \gamma_0 + \gamma_1' \mathbf{x}_t$, with

$$\gamma_0 = 0, \quad \text{and} \quad \gamma_1 = [0, 0, 0, 0, 0, 0, 0, 1, \mathbf{a}', 0]'.$$

To price nominal bonds, one can use Lemma 1 with:

$$\dot{a} = 0, \quad \dot{b} = \mathbf{0}, \quad a = \delta_0 = 0, \quad \mathbf{b} = \tilde{\delta}_1 = [0, 1, 0, \dots]', \tag{IV.1}$$

and using the risk-neutral dynamics of $\mathbf{x}_t$, characterized by (6) and (7). (That is, in Lemma 1, replace $\boldsymbol{\mu}$ and $\boldsymbol{\Phi}$ with $\boldsymbol{\mu}^{\mathbb{Q}}$ and $\boldsymbol{\Phi}^{\mathbb{Q}}$.

Indeed, with the notations a, $\mathbf{b}$, $\dot{a}$, $\dot{\mathbf{b}}$ introduced in (IV.1), we have:

$$i_t + i_{t+1} + \cdots + i_{t+h-1} = \underbrace{\max(a + \mathbf{b}'\mathbf{x}_{t+1}, 0)}_{=i_t} + \underbrace{\max(a + \mathbf{b}'\mathbf{x}_{t+2}, 0)}_{=i_{t+1}} + \cdots + \underbrace{\max(a + \mathbf{b}'\mathbf{x}_{t+h}, 0)}_{=i_{t+h-1}}. \tag{IV.2}$$

Then, in particular,

$$\begin{aligned} & \mathbb{E}_t(\exp(-i_t - i_{t+1} - \cdots - i_{t+h-1})) \\ = \; & \mathbb{E}_t(\exp(-\underbrace{\max(a + \mathbf{b}'\mathbf{x}_{t+1}, 0)}_{=i_t} - \underbrace{\max(a + \mathbf{b}'\mathbf{x}_{t+2}, 0)}_{=i_{t+1}} - \cdots - \underbrace{\max(a + \mathbf{b}'\mathbf{x}_{t+h}, 0)}_{=i_{t+h-1}})). \end{aligned}$$

To price real bonds, one can use Lemma 1 with:

$$\dot{a} = \gamma_0 = 0, \quad \dot{\mathbf{b}} = -\gamma_1, \quad a = \delta_0 = 0, \quad \mathbf{b} = \tilde{\delta}_1 = [0, 1, 0, \dots]'. \tag{IV.3}$$

Indeed, with the notations a, $\mathbf{b}$, $\dot{a}$, $\dot{\mathbf{b}}$ introduced in (IV.3), we have:

$$\begin{aligned} & (i_t - \pi_{t+1}) + (i_{t+1} - \pi_{t+2}) + \cdots + (i_{t+h-1} - \pi_{t+h}) \\ = \; & \underbrace{\max(a + \mathbf{b}'\mathbf{x}_{t+1}, 0)}_{=i_t} + \cdots + \underbrace{\max(a + \mathbf{b}'\mathbf{x}_{t+h}, 0)}_{=i_{t+h-1}} + \\ & \underbrace{\dot{a} + \dot{\mathbf{b}}'\mathbf{x}_{t+1}}_{=-\pi_{t+1}} + \cdots + \underbrace{\dot{a} + \dot{\mathbf{b}}'\mathbf{x}_{t+h}}_{=-\pi_{t+h}}. \end{aligned} \tag{IV.4}$$

V. Additional figures

Figure E.9: **Observed and fitted survey expectations**. This figure shows the model fit of surveys. Survey data are from the Federal reserve Bank of Philadelphia website (https://www.philadelphiafed.org/surveys-and-data/data-files). The forecasts are averages of expected future growth rates (for inflation and GDP) or the 3-month T-Bill rate (for the interest rate forecasts) over the considered horizon. The shaded areas represent the fitted estimates $\pm$ 2 standard deviations (using the standard errors of the measurement errors).

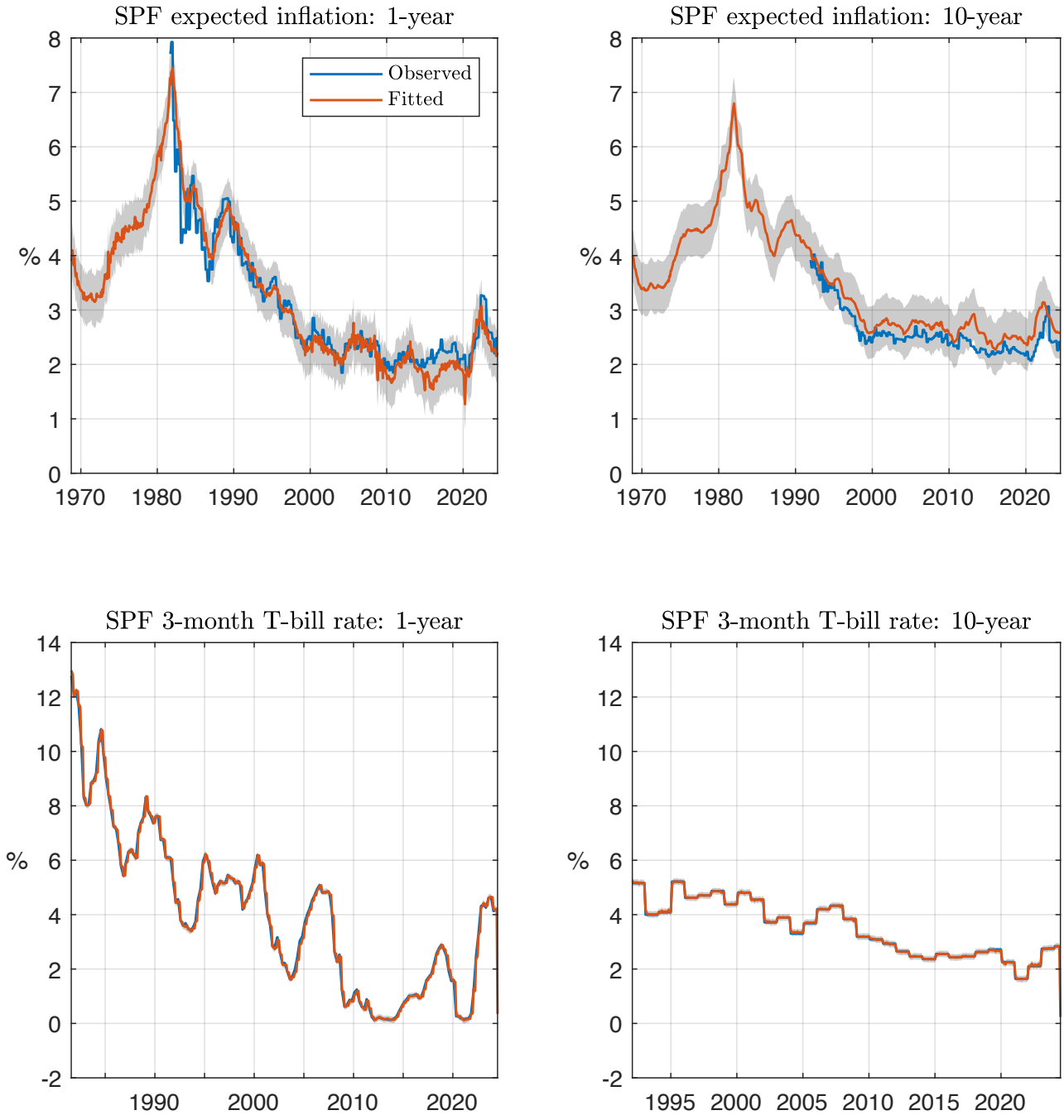

Figure E.10: **Observed and fitted nominal yields**. This figure shows the model fit of nominal yields. Except for the 3-month nominal rate (DTB3 in FRED), nominal yields are from the Federal Reserve Board website (https://www.federalreserve.gov/data/yield-curve-models.htm). These data are based on updates of Gürkaynak et al. (2007). The shaded areas represent the fitted estimates $\pm$ 2 standard deviations (using the standard errors of the measurement errors).

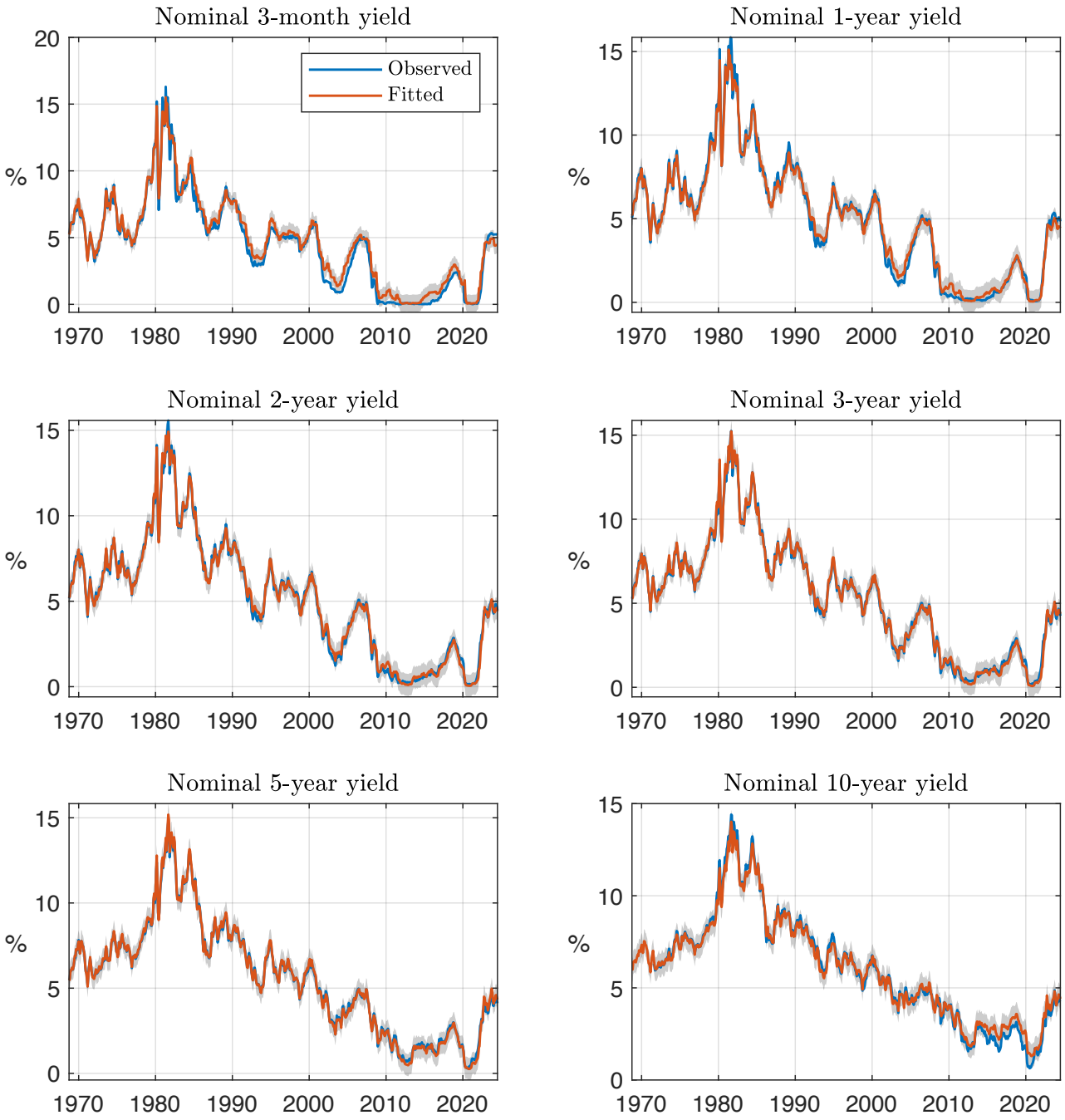

Figure E.11: **Observed and fitted real yields**. This figure shows the model fit of real yields. These data are based on updates of Gürkaynak et al. (2010). The shaded areas represent the fitted estimates $\pm$ 2 standard deviations (using the standard errors of the measurement errors).

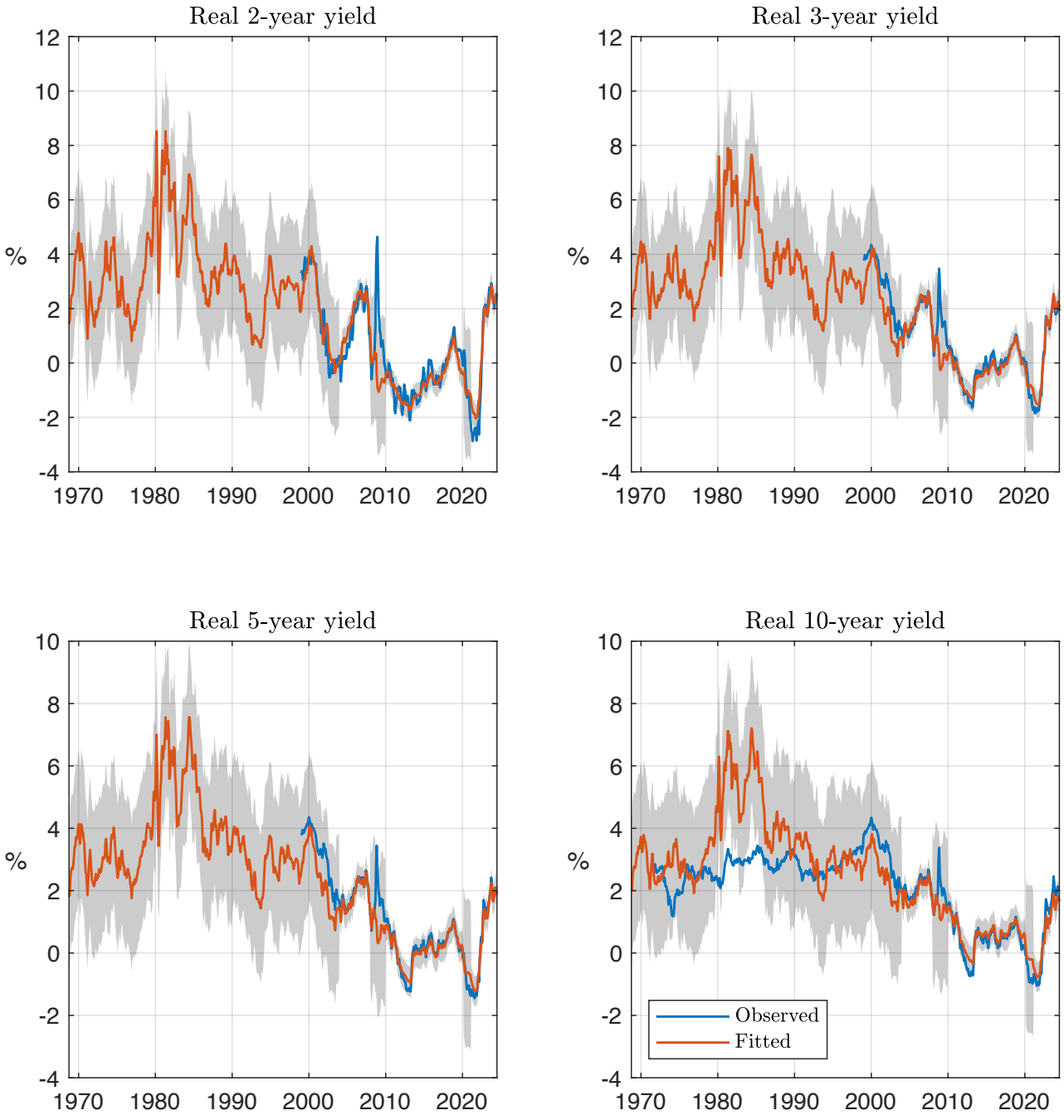

Figure E.12: **Responses of yields to monetary policy shocks ($\varepsilon_{i,t}$), conditional on r^*.** This figure shows the impulse response functions of nominal and real yields to a tightening monetary policy shock (increase in the shadow rate by 25 basis points, via $\varepsilon_{i,t}$, see eq. 14) when we are initially close to the zero-lower bound ($i_t = s_t = 0\%$), conditional on the initial value of the nominal equilibrium rate (r_t^*). It shows that yields are slightly less responsive when r_t^* is low.

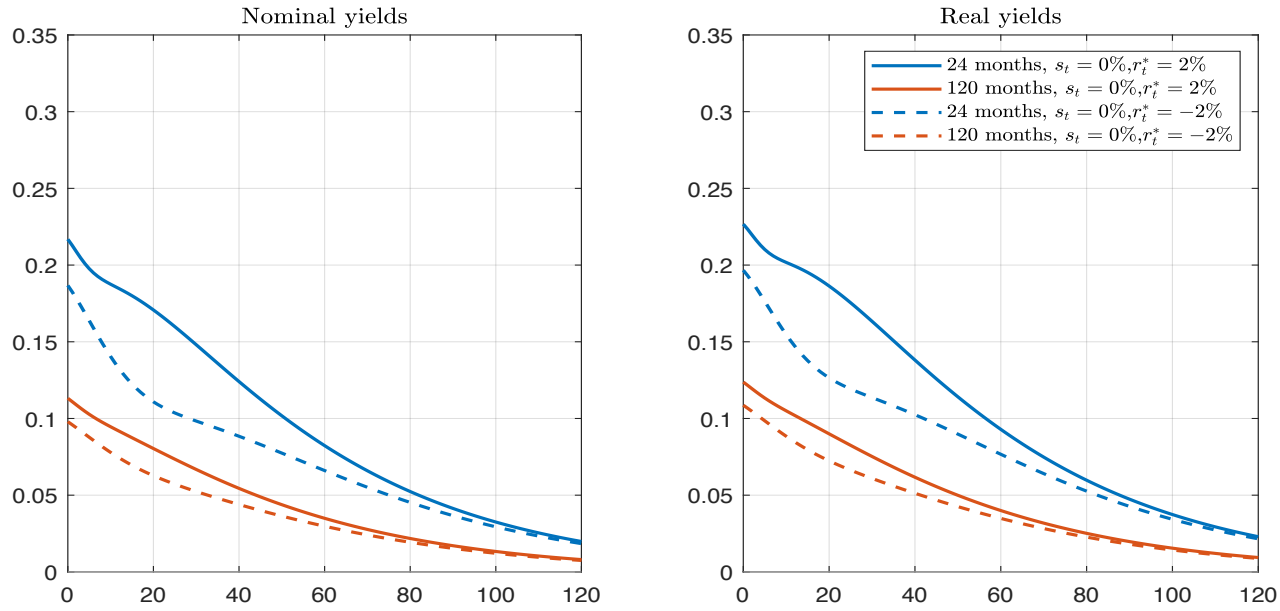

Figure E.13: **Responses of yields to monetary policy shocks ($\varepsilon_{i,t}$), conditional on r^*.** This figure shows the impulse response functions of nominal and real yields to an accommodative monetary policy shock (decrease in the shadow rate by 25 basis points, via $\varepsilon_{i,t}$, see eq. 14) when we are initially close to the zero-lower bound ($i_t = s_t = 0.25\%$), conditional on the initial value of the equilibrium nominal rate ($r_t^* + \pi_t^*$). It shows that yields are slightly less responsive when $r_t^* + \pi_t^*$ is low.

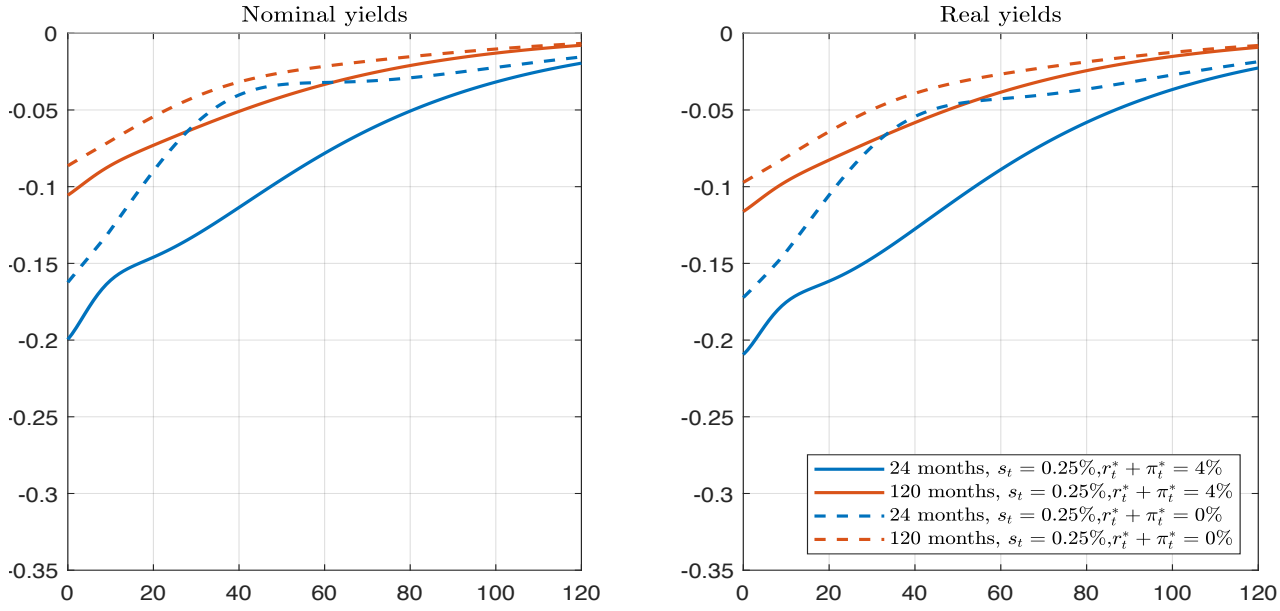

Figure E.14: **Federal funds rate and the estimated shadow rate**. This figure shows the effective federal funds rate together with the estimated shadow rate (s_t). The shaded area corresponds to the 95% confidence interval (reflecting filtering uncertainty).